



**HAL**  
open science

## Stability of Fluid Ultrathin Polymer Films in Contact with Solvent-Loaded Gels for Cultural Heritage

Amélie Castel, Philipp Gutfreund, Bernard Cabane, Yahya Rharbi

► **To cite this version:**

Amélie Castel, Philipp Gutfreund, Bernard Cabane, Yahya Rharbi. Stability of Fluid Ultrathin Polymer Films in Contact with Solvent-Loaded Gels for Cultural Heritage. *Langmuir*, 2020, 36 (42), pp.12607-12619. 10.1021/acs.langmuir.0c02162 . hal-03064935

**HAL Id: hal-03064935**

**<https://hal.science/hal-03064935v1>**

Submitted on 7 Jan 2021

**HAL** is a multi-disciplinary open access archive for the deposit and dissemination of scientific research documents, whether they are published or not. The documents may come from teaching and research institutions in France or abroad, or from public or private research centers.

L'archive ouverte pluridisciplinaire **HAL**, est destinée au dépôt et à la diffusion de documents scientifiques de niveau recherche, publiés ou non, émanant des établissements d'enseignement et de recherche français ou étrangers, des laboratoires publics ou privés.

This document is confidential and is proprietary to the American Chemical Society and its authors. Do not copy or disclose without written permission. If you have received this item in error, notify the sender and delete all copies.

**Stability of fluid Ultrathin Polymer Films in contact with solvent-loaded Gels for Cultural Heritage**

Journal:	<i>Langmuir</i>
Manuscript ID	la-2020-02162v.R1
Manuscript Type:	Article
Date Submitted by the Author:	18-Sep-2020
Complete List of Authors:	Castel, Amelie; Institut Laue-Langevin; Universite Grenoble Alpes, Laboratoire Rheologie et Procedes Gutfreund, Philipp; Institut Laue-Langevin, Cabane, Bernard; ESPCI ParisTech, PMMH rharbi, yahya; Universite Grenoble Alpes, Laboratoire Rheologie et Procedes

SCHOLARONE™  
Manuscripts

# Stability of fluid Ultrathin Polymer Films in contact with solvent-loaded Gels for Cultural Heritage

Amélie Castel,<sup>†,‡</sup> Philipp Gutfreund,<sup>\*,†</sup> Bernard Cabane,<sup>¶</sup> and Yahya Rharbi<sup>\*,‡</sup>

<sup>†</sup>*Large Scale Structure, Institut Laue-Langevin, Grenoble, France*

<sup>‡</sup>*Laboratoire de Rhéologie et Procédés, Grenoble, France*

<sup>¶</sup>*ESPCI Paris Tech, Paris, France*

E-mail: gutfreund@ill.fr; yahya.rharbi@univ-grenoble-alpes.fr

## Abstract

The removal of ultrathin amorphous polymer films in contact with an aqueous gelled solution containing small amounts of good solvent is addressed by means of specular and off-specular neutron reflectometry. The distribution of heavy water and benzyl alcohol is revealed inside Laropal®A81, often employed as a protective varnish layer for Culture Heritage in restoration of easel paintings. The swelling kinetics, interface roughness and film morphologies were recorded as a function of temperature and increasing benzyl alcohol concentration in the dispersion of Pemulen TR-2, a hydrophobically modified acrylic acid copolymer. The addition of small amounts of good solvent results in the appearance of water-filled cavities inside the varnish, which grow with time. It is shown that while increasing the solvent concentration greatly enhances the hole growth kinetics an increase in temperature above the glass transition temperature has not such a big effect on the kinetics.

## Introduction

Removing protecting thin glassy polymer films from a substrate is a critical step for numerous applications such as photonic band-gap materials,<sup>1</sup> microelectronics,<sup>2</sup> nanolithography<sup>3</sup> and lab-on-chip devices.<sup>4</sup> It is also a particularly crucial step in the restoration of easel paintings and the one bearing the highest risk. Indeed, all surfaces of old paintings and many surfaces of the contemporary paintings are covered by polymer films (varnish) which act as a protecting barrier for the pictorial layer against environmental exposure. However, due to natural ageing, external and environmental factors (dirt, light, humidity) these layers undergo irreversible changes over time. Consequently, the aesthetic and artistic aspects of the pieces of art change irreversibly due to (micro-)cracks, colour changes, oxidation, etc.

Hence regular restoration of the altered varnish layer is needed. A Common restoration procedure consists of manually transferring a good solvent to soften the altered varnish layer and mechanically removing it by abrasion. During this process, the risk of irreversible damage of the pictorial layer underneath is very high because of two factors: 1) the solvent diffusion in thin layers is difficult to control, 2) collapsing the fragile granular structure of the pictorial layer under excessive stress during manual abrasion could also lead to non visual but irreversible structural damages affecting its stability.<sup>5-10</sup> Therefore there is an urgent need to conduct precise investigations of the physical mechanisms involved during the various restoration steps.<sup>8,11,12</sup>

In order to limit the amount of aggressive solvent in the cleaning process it was proposed to work in so-called 'mild conditions' by diluting the solvent by water.<sup>13</sup> However, the results preceding this work on such binary mixtures obtained by neutron reflectometry<sup>14</sup> showed that above a solvent fraction of 0.3% the water invades the whole film through a dewetting-type process destroying the entire varnish and exposing the underlying layer to the bare liquid. On the other hand, at the beginning of the 1990s, to reduce the capillary penetration and the concentration of liquid solvents on surfaces, Wolbers suggested to increase the viscosity of the products by using polymer solutions as a matrix for the cleaning agent,

1  
2  
3 so-called Wolbers gels.<sup>15</sup> The high viscosity of the gel and the low concentration of solvent  
4 allow to reduce significantly the action of the solvent such as its penetration power. Thanks  
5 to the increase in the retention time of the products/solvents maintained in the gel matrix,  
6 the product is slowly transferred and the restorer can adapt the gel/surface contact time.  
7 Quite quickly these gels were commonly employed in cultural heritage conservation.<sup>16</sup> Gels  
8 have been widely studied since because of their applications in numerous industries such as  
9 cosmetics, food, health and even in products for safety (bulletproof vests). New innovating  
10 gels appeared, which could be suitable in art restoration like tough-gels,<sup>17</sup> micro-emulsion  
11 gels,<sup>18</sup> emulsion-gels,<sup>19</sup> and nano-gels.<sup>20</sup> In two recent reviews Baglioni *et al.* emphasize  
12 chemically cross-linked gels as a promising tool for the conservation of cultural heritage.<sup>21,22</sup>  
13 In contrast to the here studied Wolbers gels, chemical gels do not need a subsequent clean-  
14 ing after application to remove the gelling polymer residues from the surface. However,  
15 the application of gels in general and its effectiveness to remove non-original materials on a  
16 macroscopic scale are impressively demonstrated by visual images, the potential microscopic  
17 penetration of liquids into the original layers, and therefore potential irreversible changes  
18 are not investigated. In addition, after transferring a small amount of solvent by a gel into  
19 varnish, a mechanical action must follow to remove the swollen varnish. This step obviously  
20 bears risks on its own.

21  
22  
23 From a scientific viewpoint film removal seems straightforward in thick films where diffusion  
24 times and distances are macroscopic. Although the solid-to-liquid transition of polymers  
25 may be quite different from non-polymeric materials: Unlike non-polymeric materials, poly-  
26 mers do not dissolve instantaneously and the classic dissolution process of a polymer involves  
27 transport processes, namely solvent diffusion and disentanglement of the polymer chains.<sup>23</sup>  
28 The first stage is penetration of a few solvent molecules that plasticize the polymer. As a  
29 result, the macromolecules can cross the polymer/solvent interface. If the molecular weight  
30 of the polymer is high enough, they will form a gel layer at the surface of the film. The  
31 next stage is the disentanglement of the macromolecules and their escape from the gel layer

1  
2  
3 into the solvent. But there are also cases where the polymer cracks before any gel layer is  
4 formed.<sup>24</sup>  
5

6  
7 In the case of ultrathin films the situation is more complex as surface effects and reduced  
8 dimensionality may effect the physical properties of the polymer such as chain conformation,  
9 glass transition temperature and polymer dynamics.<sup>25</sup> Van der Waals interactions of the  
10 substrate may also play a role for these thin films.<sup>26</sup> And, last but not least, many films  
11 may become unstable below a certain threshold thickness leading to dewetting when heated  
12 close or above their glass transition temperature ( $T_g$ ).<sup>27</sup> The phenomenon of dewetting is  
13 relatively well studied for unpolar polymer films<sup>28</sup> but systems with a significant amount of  
14 polar groups, as the case in the present study, may significantly alter the film stability.<sup>29-31</sup>  
15

16  
17 The use of a single solvent is the easiest case of polymer film dissolution. In this study,  
18 however, a binary solvent-non solvent mixture suspended in an emulsifier solution is used.  
19  
20 The case of a binary solvent without the emulsifying co-polymer was already studied before<sup>14</sup>  
21 and revealed a dewetting-type polymer film removal due to the different surface affinities of  
22 the solvents. Using viscosity-enhancing emulsifiers to promote thin film removal, as stud-  
23 ied here, generates new challenges in polymer physics and raises particularly one important  
24 question about the emulsification mechanisms in confined media. Due to the presence of the  
25 co-polymer, the matrix is now able to absorb the hydrophobic polymer layer in form of an  
26 emulsion.<sup>32,33</sup> This increases the diversity of chemical interactions in the system and may  
27 shift the solvent partitioning.  
28  
29

30  
31 Similar to our previous study<sup>14</sup> we will determine the solvent penetration inside the polymer  
32 and follow the film break-up by using specular and off-specular neutron reflectometry (NR).  
33 NR was found an effective technique that yields both structural and chemical information  
34 thanks to targeted hydrogen/deuterium (H/D) labeling. It is an ideal tool to observe the  
35 solvent penetration in real time and has already proven this in similar experiments<sup>14,34-36</sup>. It  
36 is a non-destructive and non-invasive technique for the investigation of thin polymer films,  
37 liquid/solid and liquid/liquid interfaces with a resolution of a few Ångströms. In addition  
38  
39  
40  
41  
42  
43  
44  
45  
46  
47  
48  
49  
50  
51  
52  
53  
54  
55  
56  
57  
58  
59  
60

1  
2  
3 NR can be linked to complex sample environment like cone/plate rheology<sup>37</sup> as was done  
4 here as well. In contrast to our previous study<sup>14</sup> we cannot easily complement NR by mi-  
5 croscopy as the gel cannot be removed from the film after application without destroying  
6 the system.  
7  
8  
9

10  
11 As in our previous study<sup>14</sup> we will use ultrathin ( $\sim 100$  nm) polymer films of Laropal®A81  
12 (LA), a resin commonly used as varnish on paintings, in contact with a small quantity of  
13 benzyl alcohol (BA) dissolved in a bulk aqueous solution. In the preceding study we ob-  
14 served a swelling of the varnish layer by BA penetration at small BA quantities in the water  
15 matrix and a dewetting of the varnish by appearance of holes as depicted in Fig. 1 at BA  
16 concentration above 0.3% BA at room temperature (R.T.). The dewetting process, however,  
17 showed two remarkable differences when compared to the dewetting of polymer films from  
18 solids in air: a) The wetting layer underneath the holes was unusually thick (see Fig. 1) and  
19 b) clear loss of polymer at late stages of dewetting was observed. We identified the affinity  
20 of the water matrix to the hydrophilic substrate underneath the hydrophobic polymer to be  
21 the driving force for the film instability when in contact with the BA/water binary solution.  
22 The fact that the dewetting process started only above a threshold BA concentration in wa-  
23 ter lead us to speculate about the plasticizing effect of BA inside the polymer film reducing  
24 its glass transition temperature close to room temperature initiating polymer flow. In the  
25 present study we will vary the temperature significantly above  $T_g$  to test this hypothesis.  
26  
27  
28  
29  
30  
31  
32  
33  
34  
35  
36  
37  
38  
39  
40

41 The second difference in the current study is the addition of a gelling agent to the aqueous  
42 phase: Pemulen TR-2 as proposed for varnish removal in art restoration. Unlike the earlier  
43 studied case of water/solvent mixtures the case of physical gels containing solvent is indeed  
44 used in Cultural Heritage, so the latter system is closer to the real application.  
45  
46  
47  
48

49 Finally, in order to go towards the abrasion of the swollen varnish, we will test the influ-  
50 ence of gentle mechanical stress on the system by shearing the sample in a rheometer and  
51 watching it with NR *in situ*.<sup>37</sup>  
52  
53  
54  
55  
56  
57  
58  
59  
60

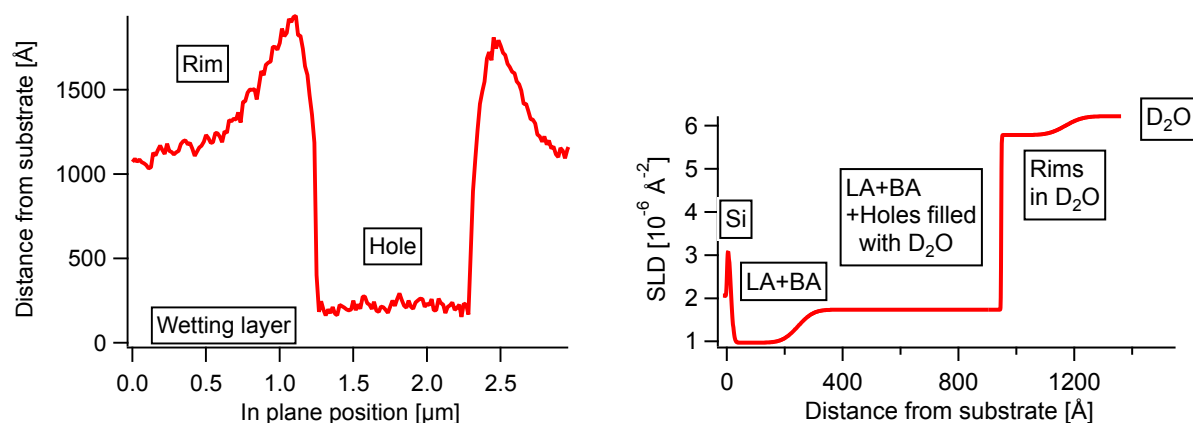


Figure 1: Left) Surface height versus in-plane position across a dewetting hole as seen by AFM in air of a LA film after prolonged exposure to a water/BA binary mixture. Right) Fitted SLD of a similar LA film in a BA/water mixture versus distance from the substrate. Note that the annealing time is longer for the AFM measurement leading to significantly larger holes and rims. This data is taken from Ref. <sup>14</sup>.

## Experimental

### Materials

Laropal®A81 (LA) from BASF<sup>38</sup> is a synthetic polymer resin synthesized from an urea, isobutyraldehyde, and formaldehyde and is a reference varnish in cultural heritage because of its stability, its resistance and transparency.<sup>39</sup> The LA structure, was reported to consist of 4-hydroxy-6-isopropyl-5,5-dimethyl-tetrahydropyrimidin-2(1*H*)-one and aldehydic compounds.<sup>40</sup> LA is a small molecular weight polymer with a typical weight-average molecular weight (Mw) of 3640 Da and number-average molecular weight (Mn) of 1266 Da as deduced from gel chromatography (GC).<sup>41</sup> The  $T_g$  measured by differential scanning calorimetry (DSC) is 48 °C.<sup>14</sup> Benzyl alcohol (Sigma-Aldrich, 99.8%), Deuterated water (D<sub>2</sub>O, Eurisotop ref D214L, 99,9% D), Pemulen TR2 (Lubrizol) and Triethanolamine (98%, CTS France<sup>42</sup>) were used as received. Pemulen TR-2 (PTR-2)<sup>32,33,43,44</sup> is an anionic polymeric emulsifier<sup>33</sup> made of a slightly crosslinked acrylic acid backbone ( $-\text{[CH}_2\text{-CH-(COOH)-]}_n\text{-}$ ) and few hydrophobic pendent alkyl molecules, 10 to 30 carbons long. It is used as a primary emulsifier and a viscosity enhancing agent<sup>45</sup>. Triethanolamine (TEA) from CTS, a



ternary amine used in cosmetic and art restoration applications is used as buffering agent for Pemulen gel preparation.

## Thin film preparation and characterization

In order to make ultrathin polymer films, LA/toluene mixtures of 20 g/L were deposited by spin coating using a Delta 6 RC TT (SÜSS MicroTec Lithography GmbH)<sup>46</sup> at 2500 RPM for 44 seconds onto silicon crystal blocks (5x5x1 cm<sup>3</sup> (111) from Sil'Tronix France or 7x7x1 cm<sup>3</sup> (100) from Crystec, Germany) rigorously cleaned following a precise protocol (20 min in deionized water, in acetone, in ethanol, in formalmyde and in water). These films were subsequently annealed at 114 ° C for 30 minutes in a vacuum oven. During this heating process, all of the toluene is evaporated and an apparent homogeneous film of LA is observed. The film thickness measured by ellipsometry are 74 nm ± 1 nm. These films did not show any apparent dewetting by optical microscopy. The films were subsequently placed in contact with different concentrations of BA (0%, 0.3%, 0.5%, 0.6% and 0.7%) in D<sub>2</sub>O with Pemulen TR-2 gel at pH 7 (adding TEA) and observed by NR as a function of shear, time and temperature.

## Preparation of the gelly matrix

The LA film was studied in contact with a polymer solution of Pemulen TR-2 from CTS France (Lubrizol). This dispersion is prepared by following the suggestions from Stravroudis<sup>44</sup> at 0.1% of PTR-2 in D<sub>2</sub>O at pH 7. First, 0.1w% dry powder of PTR-2 is mixed with water and dispersed by stirring it overnight to obtain an uniform mixture. Then, the final pH of the preparation is adjusted by adding some drops (about 0.1% in total volume) of TEA previously dissolved in D<sub>2</sub>O to the PTR-2/D<sub>2</sub>O mixture until reaching a homogeneous solution of pH 7 ± 0.2.<sup>32,44</sup> Then, a chosen amount of BA is added to the polymer solution, mixed 1 hour and left 48 hours at room temperature. At 0.1% PTR-2, the solution has a

1  
2  
3 low viscosity and it can flow through the tubing connected to the reflectometry cells.  
4  
5  
6

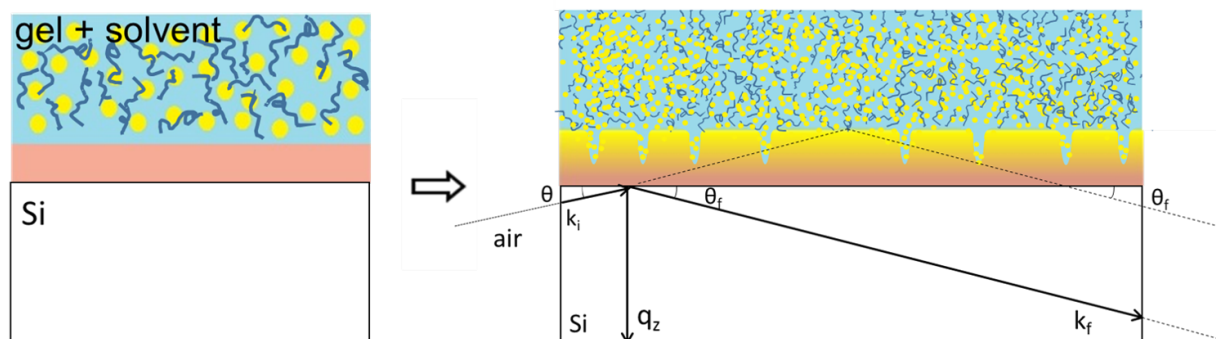
## 7 **NR experiments**

8  
9  
10 Neutron reflectometry (NR) was performed to extract the vertical swelling of the polymer film  
11 by directing a collimated neutron beam at the Si/LA/W interfaces through the Si block, and  
12 measure the reflected intensity as a function of momentum transfer normal to the interface.  
13  
14 For a short introduction of NR on the here studied system the reader is referred to our  
15 previous publication.<sup>14</sup>  
16  
17

18  
19 NR experiments were performed on the time-of-flight (ToF) reflectometer FIGARO<sup>47</sup> at the  
20 Institut Laue-Langevin (ILL), Grenoble, France. The samples were either placed in air with  
21 the neutrons reflecting up to investigate the dry polymer layer or were contained in a heated  
22 solid/liquid cell with reflection down geometry to enable potential air bubbles to drift away  
23 from the interface (see Fig. 2 for a sketch of the experiment). Some measurements were  
24 performed inside a rheometer (Anton Paar MCR501) installed *in situ* on the beam line<sup>37</sup> to  
25 impose a shear stress on the LA film during the passage of the neutron beam. This was done  
26 in reflection down geometry, as well. In all cases a wavelength band between 2 Å and 20  
27 Å was chosen with a relative wavelength resolution of 3.0% (FWHM). The detector, which  
28 allows at the same time the specular and the off specular reflectivity to be measured, has  
29 a resolution of 2.2x4.8 mm<sup>2</sup> (FWHM) and a size of 25x48 cm<sup>2</sup> at a distance of 2.8 m from  
30 the sample. The full q-range was obtained with two reflection angles of 0.622 and 2.622  
31 degrees. The beam footprint on the sample was set to 39x39 mm<sup>2</sup> for both reflection angles.  
32  
33 The raw data was normalized to the incident beam spectrum by the data reduction software  
34 COSMOS.<sup>48</sup>  
35  
36  
37  
38  
39  
40  
41  
42  
43  
44  
45  
46  
47  
48

49 Ultrathin polymer films on silicon single crystals were first placed in contact with pure D<sub>2</sub>O  
50 in order to have a reference state before swelling with BA. These films were then placed  
51 in contact with Pemulen/D<sub>2</sub>O mixture containing various fractions of BA in a closed cell.  
52  
53 Subsequently, the temperature was increased each 15 min until 70 °C and the structural  
54  
55  
56  
57  
58  
59  
60

1  
2  
3 evolution of the films was observed by NR. Four BA concentrations were studied: 0.3%,  
4  
5 0.5%, 0.6% and 0.7% BA.  
6  
7



20  
21 Figure 2: Sketch of the experiment. The yellow dots represent the solvent (BA) and the blue  
22 chains the Pemulen molecules. Note that the reflection angles are exaggerated for illustration.  
23 Also the lengths of the incoming ( $k_i$ ) and outgoing ( $k_f$ ) wave vectors are identical in elastic  
24 scattering. On the right hand side water-filled holes with finite depth inside the varnish are  
25 illustrated.  
26  
27  
28

## 29 Specular NR analysis

30  
31  
32 The measured NR data is subsequently compared to simulated NR curves calculated by an  
33 optical matrix formalism from a slab model<sup>49</sup> and the goodness of the fit is calculated. This  
34 least-squares fitting procedure is repeated until a convergence is found by using MOTOFIT.<sup>50</sup>  
35  
36 An alternative fitting program was based on a home modified Refl1D<sup>51</sup> program using python  
37 to take into account the relevance of the various parameters of the different models. The  
38 model used in all cases consists of an infinitely thick single crystal silicon slab covered by a  
39 thin layer of silicon dioxide, which thickness varied between 1 nm and 2 nm among the sam-  
40 ples, and a layer (or sequence of layers) of swollen LA/D<sub>2</sub>O/BA on top capped by an infinite  
41 layer of D<sub>2</sub>O/BA/Pemulen/TEA. Each of the slabs has three fitting parameters, the thick-  
42 ness, the roughness and the scattering length density (SLD). The SLD is the number density  
43 of isotopes per unit volume multiplied by the corresponding scattering length for neutrons.  
44  
45 It can be calculated by knowing the mass density of a material and its chemical sum formula.  
46  
47 The SLD calculator from the NIST webpage was used here which uses tabulated values for  
48  
49  
50  
51  
52  
53  
54  
55  
56  
57  
58  
59  
60

1  
2  
3 scattering lengths and isotope weights.<sup>52</sup> The SLDs and the corresponding chemical sum  
4 formulas used in this study can be found in Tab. S2 in the supporting information (SI). The  
5 thickness and the roughness of all layers were fitted as well. The silicon substrate and silicon  
6 dioxide were found to be atomically smooth (between 0.2 nm and 0.5 nm) and therefore are  
7 not discussed further.  
8  
9

10  
11  
12 Several morphological models were envisaged for the LA layer to fit the data including 1) A  
13 dewetting profile consisting of three sub-layers as shown in Fig. 1: Dry wetting layer, layer  
14 perforated by water-filled holes and a projected layer due to rims as used in our previous  
15 study about the same films in contact with BA/water,<sup>14</sup> 2) LA layers with holes that cross  
16 the films down to the substrate without a wetting nor a rim layer, 3) Similar to 2) but with  
17 limited depth holes (see Fig. 3 Bottom) and 4) a single homogeneously mixed layer consisting  
18 of LA/BA/water. Note, that models 2) and 4) cannot be distinguished by specular reflec-  
19 tometry alone, as for each of these models the SLD profile is estimated by in-plane averaging  
20 the LA and D<sub>2</sub>O fractions. The NR spectra were calculated using Motofit or Refl1D with a  
21 modified model corresponding to the morphological case, and compared to the experimental  
22 spectra using a step by step least-squares fitting procedure. In order to justify the in-plane  
23 averaging of the SLDs, the size of the defects are supposed to be smaller than the in-plane  
24 neutron coherence length.  
25  
26  
27  
28  
29  
30  
31  
32  
33  
34  
35  
36  
37  
38  
39  
40

41 Note that the scaling of the fitted reflectivity curves was fixed to one in one set of anal-  
42 ysis. The lower scaling of the measured curves at an advanced stage of layer destruction is  
43 due to enhanced off-specular scattering as explained in the Supplementary Information. In  
44 these cases the low q part of the NR curves was excluded from the fitting procedure. In  
45 another set of analysis the scaling factor was adjusted when the OSS becomes important  
46 and the low q part of the NR was also fitted. This analysis strategy lead to good fits as well,  
47 the resulting SLD values were not physically reasonable, though.  
48  
49  
50  
51  
52  
53  
54  
55  
56  
57  
58  
59  
60

In order to extract quantitatively the partial volume fractions from the NR spectra two approaches were used: First the system was simplified into only two components: The polymer with a  $SLD_{LA}$  value of  $0.9 \times 10^{-6} \text{ \AA}^{-2}$  and solvent with the fitted  $SLD_s$  values from the critical edge positions of the NR curves. From the fitted mean SLD values  $SLD$  and thicknesses  $h$  of the layer the resulting 'dry' volumes of the polymer  $v_{pol}$  (normalized to the dry LA volume) and solvent  $v_s$  fractions were extracted using the following formula:

$$v_{pol} = \frac{h(SLD - SLD_s)}{h_0(SLD_{LA} - SLD_s)} \quad (1)$$

$$v_s = \frac{h}{h_0} - v_{pol}$$

Here  $h_0$  is the dry thickness of the polymer. This approach does not assume mass conservation but can only extract two unknowns from the two measured values. Assuming conservation of the polymer mass ( $v_{LA} = 1$ ) as done in our previous work for low BA concentrations<sup>14</sup> one can extract the BA (excess) volume fraction  $\phi_{BA/LA}$  as well as the water fraction  $\phi_{W/LA}$  inside the polymer layer from the following boundary conditions:

$$1 + \phi_{W/LA} + \phi_{BA/LA} = \frac{h}{h_0} \quad (2)$$

$$\frac{h}{h_0} * SLD = \phi_{W/LA} * SLD_w + \phi_{BA/LA} * SLD_{BA}$$

$$+ \left( \frac{h}{h_0} - \phi_{W/LA} - \phi_{BA/LA} \right) * SLD_{LA},$$

where  $SLD_{BA}$  is the bulk SLD of BA.

### Off-Specular neutron reflectivity

As the neutron reflectivity spectra were recorded using 2D detectors the off specular neutron reflectivity (OSS) is also accessible.<sup>53</sup> The OSS intensity corresponds to the intensity scattered at a condition away from the mirror reflection (NR). In this case the total momentum transfer also comprises an in-plane component. This allows one to determine SLD

1  
2  
3 variations parallel to the interface but due to the geometry the momentum transfers are  
4 typically two orders of magnitude smaller than in specular reflectometry and therefore the  
5 spatial resolution is much lower probing micrometer sized structures. The 2D OSS patterns  
6 were simulated in wavelength vs. scattering angle space using the Distorted Wave Born  
7 Approximation (DWBA) assuming exponentially decaying in-plane correlation functions.<sup>54</sup>  
8 This gave access to one additional parameter, namely the mean size of in-plane inhomoge-  
9 neities.  
10  
11  
12  
13  
14  
15  
16  
17  
18  
19  
20

## 21 Results

### 22 23 24 **Film morphology in contact with BA/TR2/water gel from specular** 25 26 27 **NR analysis** 28 29

30 A first-glance analysis of the NR spectra suggests a substantial LA film swelling in contact  
31 with BA/water/pemulen (Fig. 3). In accordance with the previous study which has shown  
32 that the LA thin film dewets the Si substrate when exposed to BA/water mixtures,<sup>14</sup> one  
33 could extrapolate this process to explain the NR data in contact with BA/water/pemulen  
34 as well. Dewetting leads to holes and rims and yields typically an averaged SLD profile as  
35 depicted in Fig. 1. When, however, the NR spectra of films exposed to BA/water/pemulen  
36 are fitted in terms of this dewetting induced SLD profile with various rim morphologies  
37 (height, width and fractions), the  $\chi^2$  values were found minimum for a rim fraction equal to  
38 0 (Fig. 4). This strongly rejects rims as a potential morphology in the present case.  
39  
40  
41  
42  
43  
44  
45  
46  
47

48 The second significant difference compared to LA films immersed in only solvent/non-solvent  
49 mixtures studied previously<sup>14</sup> is the absence of a well-defined wetting layer. Only models of  
50 constant SLD profile or SLD gradients over the entire layer (no sharp SLD step, see Fig. 3)  
51 lead to reasonable  $\chi^2$  values. In all cases the growth of the average SLD of LA exposed to  
52 BA/water/pemulen is apparent resulting either from holes that cross the film, non crossing  
53  
54  
55  
56  
57  
58  
59  
60

1  
2  
3 holes or heterogeneous zones of LA/BA/water/Pemulen inside the films. These models can  
4 all reasonably fit the specular NR spectra with small variation depending on the fraction  
5 of BA and temperature. The best goodness of fit for the 0.3% BA concentration with  $\chi^2$   
6 values around 4 was achieved assuming a gradient in SLD across the whole layer starting  
7 with the SLD value of the polymer layer when in contact with pure D<sub>2</sub>O close to the Si  
8 substrate and an increasing SLD towards the aqueous phase. This profile corresponds to a  
9 distribution of hole depths with only few reaching the Si substrate (penetrating the whole  
10 film). Typical reflectivity fits and SLD profiles using this model can be seen in Fig. 3. For  
11 higher BA concentrations, in addition to the gradient, the SLD of the LA in contact with Si  
12 had to be fitted as well to reach similar  $\chi^2$  values. This resulted in flat SLD profiles inside  
13 LA corresponding to water-filled holes crossing the whole film. A typical NR fit in this case  
14 can be seen in Fig. 4.  
15  
16  
17  
18  
19  
20  
21  
22  
23  
24  
25  
26

27 If the scaling factors of the NR data were adjusted in the fit, qualitatively similar results  
28 were obtained particularly for the total film thickness, however, the absolute SLD values  
29 gave nonphysical results.  
30  
31  
32  
33  
34  
35  
36  
37  
38  
39  
40  
41  
42  
43  
44  
45  
46  
47  
48  
49  
50  
51  
52  
53  
54  
55  
56  
57  
58  
59  
60

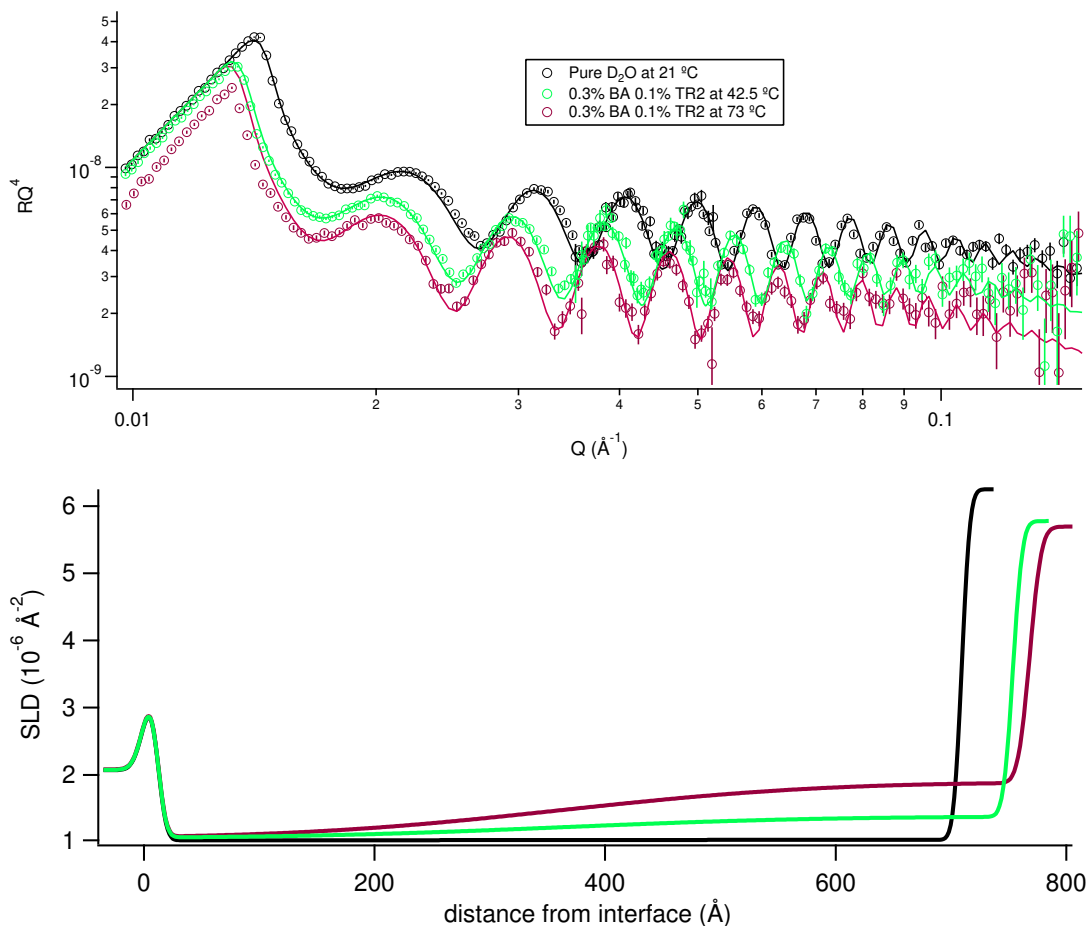


Figure 3: Top) Typical reflectivity curves (multiplied by  $q_z^4$ ) vs. momentum transfer  $q_z$  on a logarithmic scale for LA films in pure  $D_2O$  (black circles) and in aqueous solutions of 0.3% BA and 0.1% Pemulen at two different temperatures as depicted in the legend. The solid lines in the same color code are fits to the data. Bottom) The corresponding SLD profiles in the same color code.



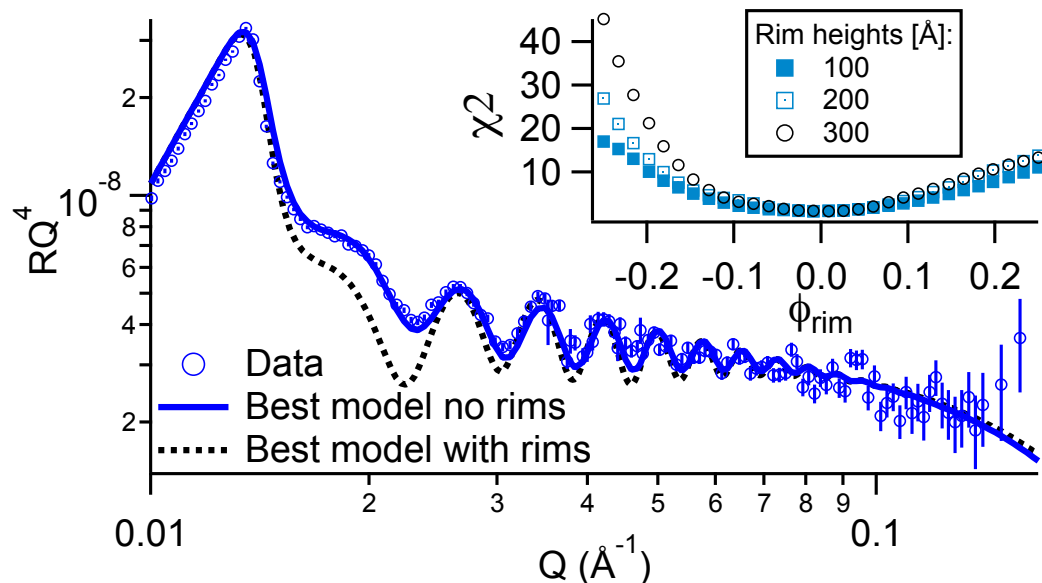


Figure 4: Reflectivity curve (multiplied by  $q_z^4$ ) vs. momentum transfer  $q_z$  on a logarithmic scale for an LA film in aqueous solutions of 0.5% BA and 0.1% Pemulen at 27°C (data points). The solid line in the same color code is the best fit to the data assuming no rims. The broken line is the best fit to the data assuming a rim fraction as in Fig. 1 left. Inset: Normalized least square value  $\chi^2$  vs. fraction of rims  $\phi_{rim}$  for various heights of rims as indicated in the legend deduced from fitting the specular NR spectra to a model of LA containing a fraction of holes and rims.

## Effect of temperature and BA concentration on film swelling in BA/pemulen/D<sub>2</sub>O gel

Fig. 5 shows significant swelling of LA films when exposed to BA/Pemulen/D<sub>2</sub>O gels for all the cases investigated here. For the case of 0.3%, the swelling ratio (SWR) is calculated as the ratio of the film thickness in the presence of BA/Pemulen/water to that in pure D<sub>2</sub>O. This is justified by the fact that LA films do not swell in the presence of pure D<sub>2</sub>O even after 24 h at least within the resolution of the NR experiment.<sup>14</sup> At room temperature (21 °C), Fig. 5 shows that the LA film swells by 4.5% at a BA concentration of 0.3% which is the exact same swelling ratio found without the gel.<sup>14</sup> D<sub>2</sub>O is unlikely to swell LA films to the extent to be measurable by NR because the Flory-Huggins interaction parameter  $\chi_{LA/D_2O}$  exceeds 4 at room temperature and therefore can safely be excluded as the swelling molecule.<sup>14</sup> LA

swelling in BA/Pemulen/D<sub>2</sub>O is most likely due to BA which has a favorable Flory-Huggins interaction parameter  $\chi_{BA/LA}$  between -0.05 and 0.17.<sup>14</sup> Because of its high molecular weight Pemulen can also be excluded as a swelling agent for LA. Even if TEA can swell LA, it is unlikely to account for the measured LA swelling in the present case because it is highly miscible in water. Even in the extreme case of a similar interaction parameter with water ( $\chi_{W/TEA}$ ) and LA ( $\chi_{LA/TEA}$ ), the partitioning of TEA in LA would not exceed the concentration of TEA in water, which is 0.1%, which is within the error bar of the measured SWR. Therefore one can safely attribute the measured SWR to BA uptake by the LA film.

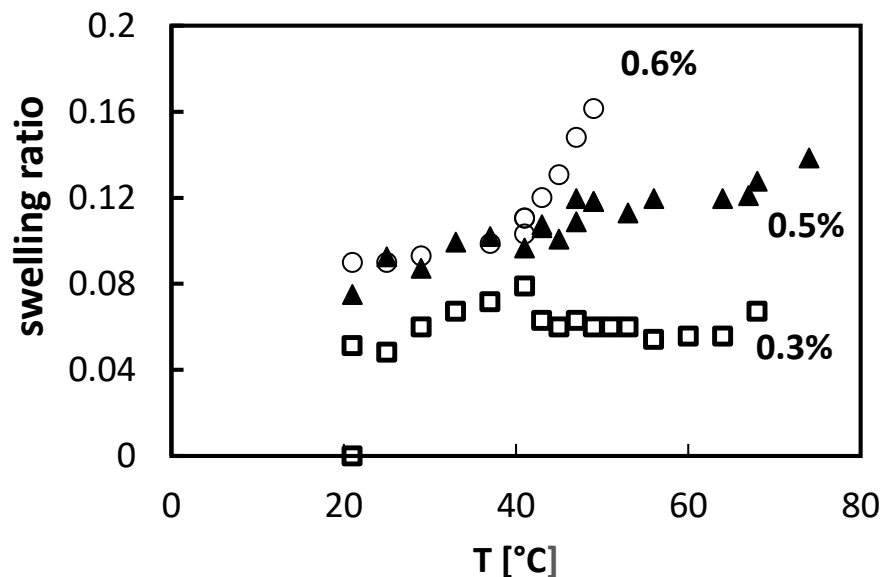


Figure 5: Swelling ratio of a LA film in BA/PTR2/water vs. temperature for BA fractions of 0.3%, 0.5% and 0.6%. The swelling ratio is calculated as the ratio of the film thickness in the presence of BA/PTR2/D<sub>2</sub>O at various temperatures to the initial film thickness in pure D<sub>2</sub>O. The thickness is extracted from the analysis of NR spectra. For 0.5% and 0.6% the film thickness is extrapolated from dependence of the swelling ratio on  $\phi_{Ba/W}$  and film thickness at room temperature.

In order to extract the individual partitions of the involved materials the volume fractions of two constituents can be extracted if the polymer mass conservation is not imposed (eq. 1) or three constituents if the conservation of polymer mass is assumed (eq. 2) from the fitted

NR curves with a two-polymer-layer model as described in the Experimental section. The resulting total volumes of solvent and polymer within the layer without imposing polymer mass conservation are plotted in Fig. 6.

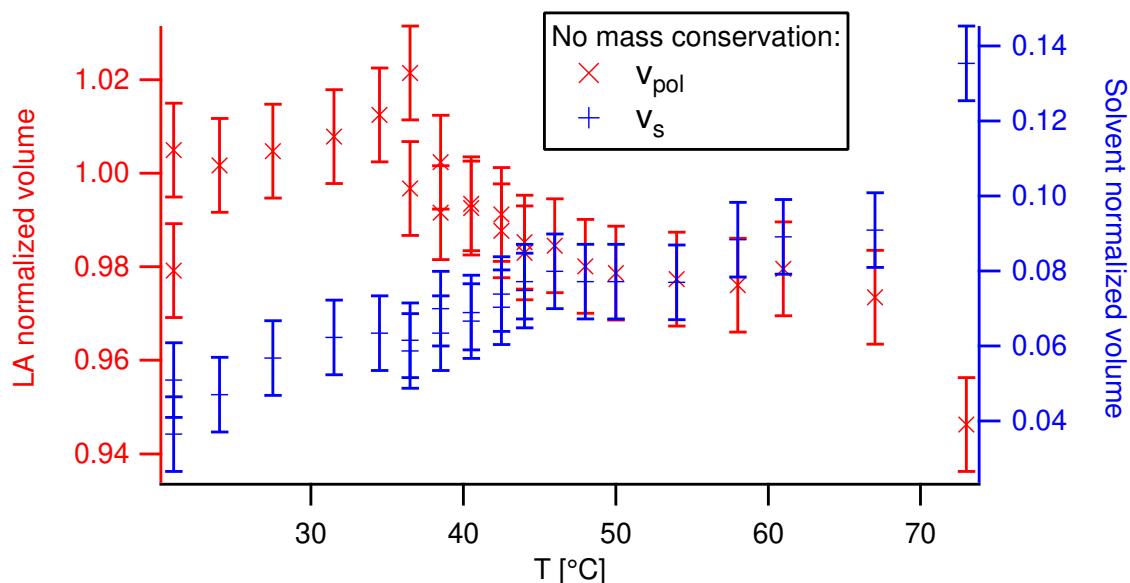


Figure 6: Normalized (excess) volumes of the polymer (red x-crosses, left axis) and liquid (blue crosses, right axis) inside the LA layer from NR of 0.3% BA and 0.1% PTR-2 in  $D_2O$  according to the boundary condition eq. 1 as a function of temperature. Note: The two points at R.T. for each fraction were measured at two different times, once at the very beginning and a second time after heating to  $40^\circ C$  indicating that the polymer loss is irreversible, but the solvent penetration is reversible within error.

As can be seen in the graph the polymer mass seems to be conserved until  $38^\circ C$  with an increasing solvent fraction with temperature. Above this temperature there is clearly (irreversible) loss of polymer observed on the expense of more and more solvent penetrating the film. Therefore below this temperature the mass conservation can be assumed and a more detailed partial swelling can be extracted differentiating between water and BA (eq. 2). This result is presented in Fig. 7.

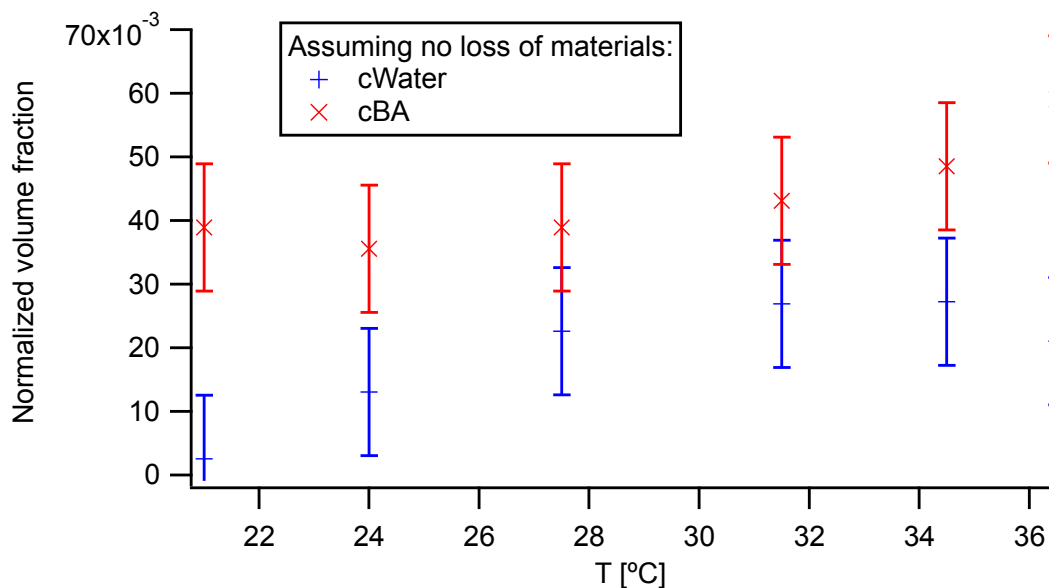


Figure 7: Normalized volume fractions of BA (red x-crosses) and water (blue crosses) from NR of 0.3% BA and 0.1% PTR-2 in D<sub>2</sub>O according to the boundary condition eq. 2 as a function of temperature.

As suggested above from the Flory-Huggins interaction parameters indeed the swelling at R.T. is mainly attributed to BA with no significant penetration of water. However, with increased temperature (and time) it seems that the volume fractions of both water and BA are increasing. It has to be noted, however, that the increase in BA fraction with temperature is reversible but the water fraction increase is not. Therefore it seems that there are two parameters influencing the partitions: Increased chemical compatibility of BA and LA with temperature and onset of dewetting by water filled cavities with time.

The fact that the presence of hydrophobic domains from the Pemulen TR2 side group (C10 to C30) does not shift the partitioning balance of BA or water is an important result as Pemulen effectively acts as an emulsifier. This could only infer that the number of hydrophobic moieties at this PTR2 concentration of 0.1% is not enough to perturb the swelling equilibrium. Recovering the same SWR with or without Pemulen at room temperature for 0.3% is a first important result for restoration processes as this means that there is no need to increase the BA concentration when using Pemulen to control solvent transfer to the varnish layer at least when working at room temperature.

1  
2  
3  
4  
5  
6  
7  
8  
9  
10  
11  
12  
13  
14  
15  
16  
17  
18  
19  
20  
21  
22  
23  
24  
25  
26  
27  
28  
29  
30  
31  
32  
33  
34  
35  
36  
37  
38  
39  
40  
41  
42  
43  
44  
45  
46  
47  
48  
49  
50  
51  
52  
53  
54  
55  
56  
57  
58  
59  
60

Whatever the exact model used for fitting the specular NR of LA in BA/PTR2/D<sub>2</sub>O, a SLD growth with temperature (and time) of the LA film is observed, which can only suggest D<sub>2</sub>O invasion into the LA film as it is the largest SLD constituent as quantitatively shown above. The film invasion with water can result either from creation of penetrating or non-penetrating holes filled with D<sub>2</sub>O or formation of LA/BA/D<sub>2</sub>O mixed zones. Assuming holes as the reason for increased water fractions it is possible to calculate SLD density profiles by assuming a Gaussian distribution of cylindrical water filled holes around a mean depth inside a LA film of fitted total thickness. The detailed analysis of the NR spectra with this model assuming LA mass conservation using the least square method yields similar tendencies for the dependence of the surface fraction of holes ( $\phi_{hole}$ ) on temperature for fully penetrating holes and for holes with finite depth (see Fig. 8).  $\phi_{hole}$  was found to increase slightly for 0.3% with increasing the temperature up to 70 °C. On the other hand  $\phi_{hole}$  for 0.5% strongly increase up to the breaking temperature and for 0.6% increases rapidly between 37 °C up to the breaking temperature of 49 °C. The absolute values of  $\phi_{hole}$  are higher if the LA mass is allowed to decrease, but the qualitative trend stays the same. We will therefore present the SLD of the fitted LA layer rather than  $\phi_{hole}$  in the following in order to be less model dependent.

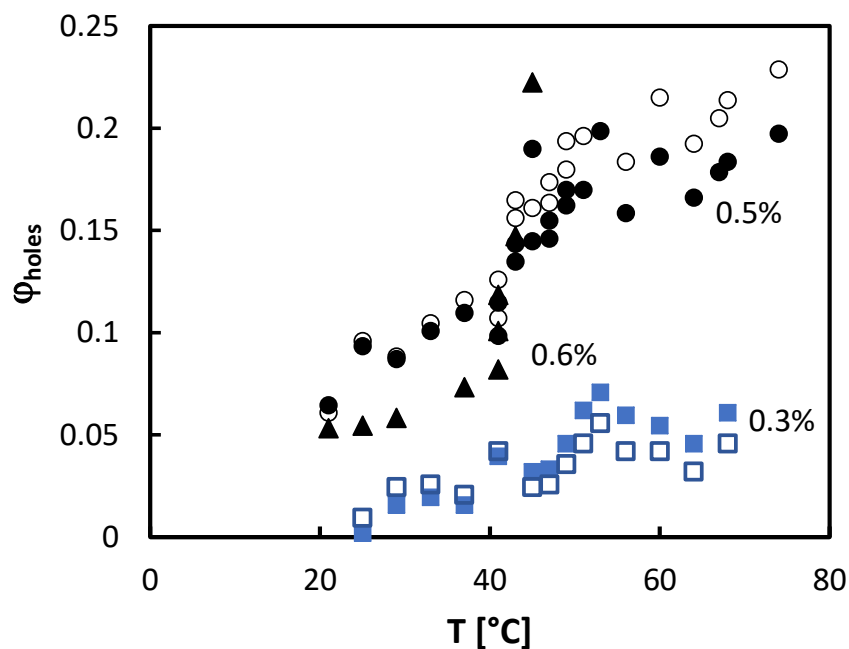


Figure 8: Surface fraction of holes ( $\phi_{hole}$ ) containing  $D_2O$  vs. temperature for films in contact with BA/PTR2/ $D_2O$  for BA fraction of 0.3%, 0.5% and 0.6%.  $\phi_{hole}$  was deduced from fitting the NR spectra to a crossing hole model (full symbols) and non-crossing holes (empty symbols).

## Effects of temperature and BA concentration on the film heterogeneities prior to film breaking in the BA/pemulen/ $D_2O$ dispersion

Many aspects of the reflectively spectra of Laropal®A81 in BA/pemulen/ $D_2O$  point out to the initiation and evolution of significant heterogeneities and defects. This can be seen in the off-specular scattering, film roughness and the process of water invasion. From the first glance, these defects could be analyzed in terms of a simple dewetting process induced by BA as in the case BA/ $D_2O$  (without Pemulen). However, significant morphological differences to the case in pure are observed and will be discussed in the following.

### Film heterogeneities from OSS

1  
2  
3  
4  
5  
6 In all NR measurements a clear Yoneda-type scattering was observed around the critical  
7 momentum transfers (see Fig. 9). This points towards in-plane SLD correlations present in  
8 the system. Quantitative fits of the 2D scattering patterns<sup>54</sup> clearly showed that the origin  
9 of this scattering comes from inhomogeneities inside the bulk of the film filled with water.  
10 The interface roughness as the only origin of the scattering can be clearly excluded as this  
11 would lead to much less scattered intensity. Moreover, it became evident that the SLD con-  
12 trast contributing to this scattering must come from D2O rich phases inside the polymer,  
13 which is the largest SLD contrast when looking at Table S2 in the supporting information.  
14 This bares striking similarities to our previous study of LA films in binary water/BA mix-  
15 tures,<sup>14</sup> where water-filled holes were the origin of the OSS scattering as evidenced by AFM.  
16 In the present case AFM measurements were not possible as the gelly solution was sticking  
17 to the polymer films and impossible to be removed without detachment of the LA film as well.  
18  
19  
20  
21  
22  
23  
24  
25  
26  
27  
28  
29  
30  
31  
32  
33  
34  
35  
36  
37  
38  
39  
40  
41  
42  
43  
44  
45  
46  
47  
48  
49  
50  
51  
52  
53  
54  
55  
56  
57  
58  
59  
60

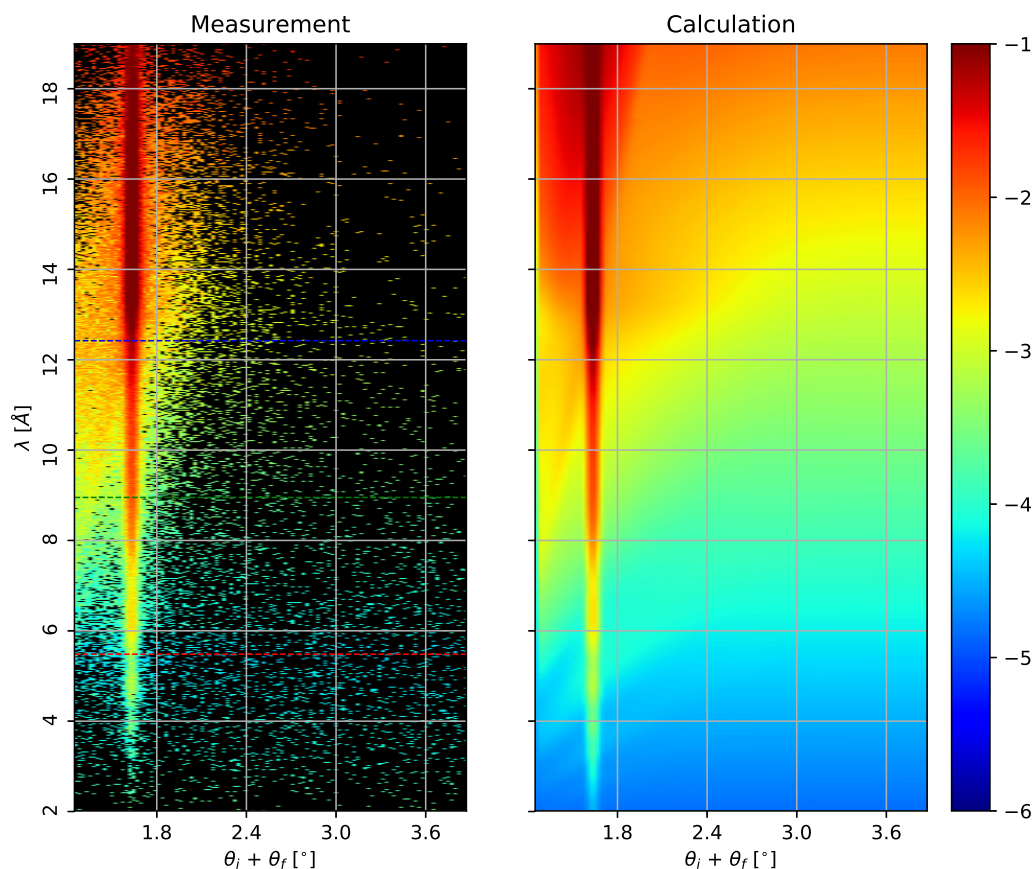


Figure 9: Left: OSS of a LA film in contact with 0.3% BA and 0.1% PTR-2 in  $D_2O$  at  $72^\circ C$ . Right: Simulation using the same instrument parameters as in the measurement and using the fitting results from the specular fits and in-plane inhomogeneities filled with water assumed to follow an exponentially decaying SLD on average with a characteristic length of  $0.7 \mu m$ .

From the quantitative fits of the OSS intensity to an exponentially decaying in-plane SLD inhomogeneity one can extract a characteristic in-plane correlation length, which would correspond to an average hole radius in case of holes. This is plotted in Fig.10 for a 0.5% BA solution in 0.1% Pemulen as a function of temperature. In addition the SLD from the specular fits is shown on the same graph. In order to put these results into perspective with



1  
2  
3 the pure water case the results from a similar LA film in contact with a 0.5% BA solution  
4 in pure water are added to the graph. These are from the preceding study done at room  
5 temperature only.<sup>14</sup> Here another apparent difference between the varnish in contact with a  
6 gel and with pure water, both containing BA, can be appreciated: While the SLD is on the  
7 same order for both cases at low temperatures it clearly increases significantly for the gelly  
8 case at elevated temperatures. The SLD increase is linearly related to the volume fraction  
9 of water-filled holes inside the layer, which means that the volume fraction of holes is signif-  
10 icantly higher in the Pemulen solution at elevated temperatures compared to the pure water  
11 case at R.T. On the other hand the size of the holes is smaller in the case of the polymer  
12 dispersion, even at the highest temperature investigated here. This unambiguously testifies  
13 a significantly higher hole density in the case of the Pemulen solution. Assuming the hole  
14 size extracted from the quantitative OSS fits to be the hole radius, the hole density at R.T  
15 for 0.5% BA in pure water is about  $0.1 \mu\text{m}^{-2}$  and for the same BA concentration inside the  
16 Pemulen solution at  $49^\circ\text{C}$  is about  $3 \mu\text{m}^{-2}$  if the holes are not overlapping.  
17  
18  
19  
20  
21  
22  
23  
24  
25  
26  
27  
28  
29  
30  
31  
32  
33  
34  
35  
36  
37  
38  
39  
40  
41  
42  
43  
44  
45  
46  
47  
48  
49  
50  
51  
52  
53  
54  
55  
56  
57  
58  
59  
60

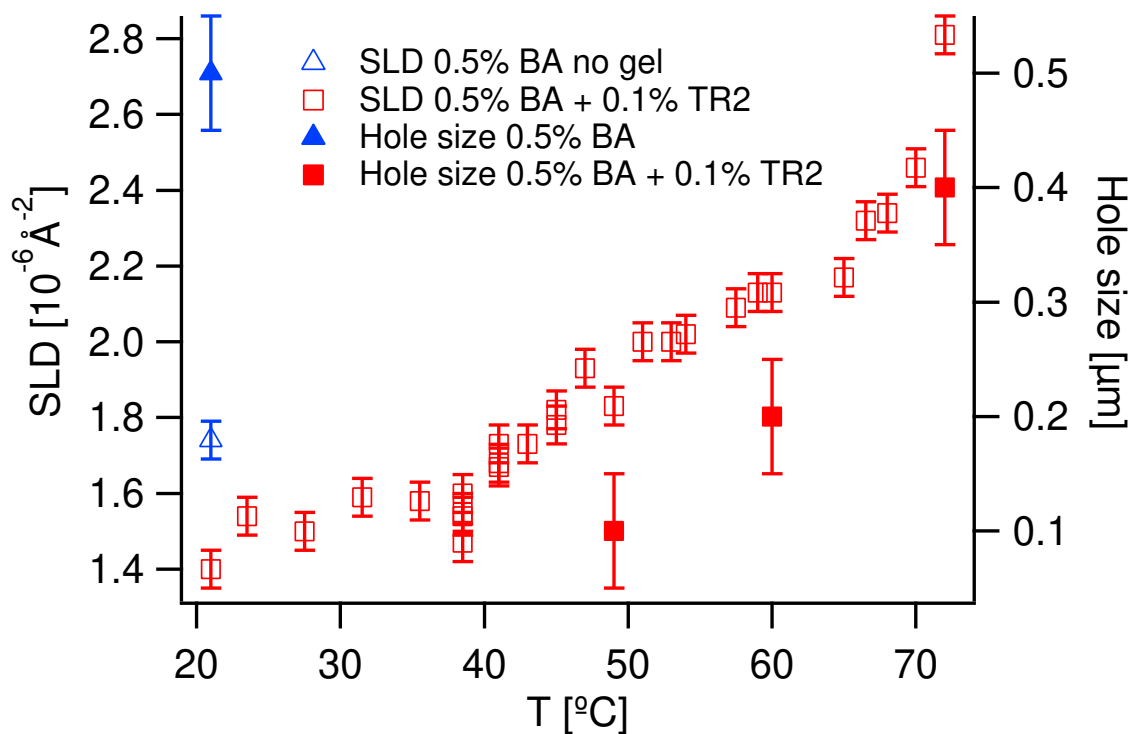


Figure 10: Left axis: SLD as a function of temperature from a LA polymer film in contact with 0.5% BA and 0.1% PTR-2 in D<sub>2</sub>O (open squares). Right axis: Extracted hole radius from the OSS simulations of the same sample (filled squares). The triangles correspond to the SLD (open triangle) and the hole radius (filled triangle) of a LA film in contact with a 0.5% BA solution in pure D<sub>2</sub>O after 2 h immersion.

### Interface between varnish films and PTR2/BA aqueous solutions

The microscopic roughness of the polymer/liquid interface deduced from NR analysis is found to be around 0.6 nm at room temperature and low BA concentrations, while increasing to up to 1.2 nm at higher temperatures or BA concentrations. These values are manifestly higher than the reported one in the case of binary BA/D<sub>2</sub>O mixture<sup>14</sup> which never exceeded 0.3 nm. This suggests that adding Pemulen into the aqueous phase favors surface roughness.

An immiscible polymer/polymer interface should develop an interface width  $\sigma$  corresponding to the squared sum of the intrinsic roughness  $\sigma_i$  coming from chemical interactions and scaling with the monomer size  $a$ ,<sup>55</sup> and the capillary wave roughness  $\sigma_{CW}$  due to interfacial tension

1  
2  
3  $\gamma$  if the sample is in equilibrium<sup>56</sup>:  
4  
5

$$6 \quad \sigma^2 = \frac{k_B T}{2\pi\gamma} \ln\left(\frac{l_c}{a}\right) + \sigma_i^2, \quad (3)$$

7  
8  
9  
10 where the capillary wave spectrum is cut by the neutron coherence length  $l_c$ .  $k_B$  denotes the  
11 Boltzmann constant. The intrinsic width for a high Flory-Huggins interaction parameter  $\chi$   
12 can be estimated by<sup>55</sup>:  
13  
14

$$15 \quad \sigma_i = \frac{a\sqrt{N}}{3\sqrt{\chi/2 * N - 1}}, \quad (4)$$

16  
17  
18 with the polymerization  $N$ . The surface energy of Laropal®A81 was determined by mea-  
19 suring the contact angle of different liquids on top of a macroscopic LA film<sup>57</sup> and turned  
20 out to be around 30 mN/m.  
21  
22

23 Using water as the "monomer" with a typical size of a water molecule of 1.8 Å<sup>58</sup> one gets in-  
24 deed around 3 Å roughness of the interface using the  $\chi$  values between 2.5 and 4 and  $N = 30$   
25 as determined in our previous study<sup>14</sup>. Using around 1 nm as the size of the monomer results  
26 in roughness between 4.5 Å and 5.5 Å for the binary mixture. In the case of the lower sur-  
27 face tension of the gelled solvent of around 56 mN/m<sup>32</sup> we get indeed higher values between  
28 3.6 Å and 5.9 Å using 1.8 Å or 1 nm as the monomer size, respectively, assuming the same  
29  $\chi$  values as for the binary mixtures. This slight roughness increase can explain the interface  
30 width of the polymer/D2O/Pemulen system measured at R.T. which is around 6 Å for 0.3%  
31 or 0.5% BA, especially taking account that the Pemulen acts as an emulsifier, although its  
32 volume fraction is very low (0.1%). The increase of the roughness with temperature up  
33 to 70° between 1 Å and 2 Å for the 0.3% or 0.5% BA mixtures, respectively, is, however,  
34 more than what would be expected by a mere reduction in interfacial tension with increasing  
35 temperature. Moreover, the roughness values above 1 nm in the case of 0.6% BA cannot be  
36 explained by a decreased interfacial tension alone, but have to involve a reduction of the  
37 Flory-Huggins interaction parameter as a function of temperature. This result is in accord  
38 with the increased BA swelling of LA at elevated temperature as observed in Fig. 7.  
39  
40  
41  
42  
43  
44  
45  
46  
47  
48  
49  
50  
51  
52  
53  
54  
55  
56  
57  
58  
59  
60

1  
2  
3 Interestingly the temperature induced roughness increase of the aqueous/polymer interface  
4 seems to plateau at a certain temperature as can be seen in Fig. 11. The origin of this  
5 effect remains somewhat unclear. This temperature is close to the glass transition temper-  
6 ature if calculated using the binary mixing model as will be explained later. One could  
7 therefore imagine that 'unfreezing' of stresses could be the origin of this stagnation. Note,  
8 however, that the change in roughness is reversible as the value at room temperature was  
9 measured twice at different moments during the heating protocol (see the two points at R.T.  
10 in Fig. 11). Therefore this behaviour is unlikely to be related to non-equilibrium properties.  
11 On the other hand, starting from 40 °C a loss of polymer mass is observed (see Fig. 6) by  
12 formation of water-filled cavities. It is therefore possible that the roughness contribution due  
13 to these cavities is significantly larger than the intrinsic interface roughness and therefore  
14 screens the latter as specular NR measures only the sum of the two contributions. Again,  
15 the reversibility of the roughness increase even after the appearance of cavities contradicts  
16 this hypothesis. Another possibility is that the interaction between BA and LA becomes  
17 athermal above 40 °C meaning no further improvement of the polymer/solvent compatibility  
18 at higher temperatures. A counter indication to this explanation is that in a test a LA/BA  
19 mixture (5% BA) was cooled down to -20° and showed no indication of phase separation,  
20 meaning the BA at room temperature is already far away from theta condition, also consis-  
21 tent with the very low Flory-Huggins parameter around zero.  
22  
23  
24  
25  
26  
27  
28  
29  
30  
31  
32  
33  
34  
35  
36  
37  
38  
39  
40

41 Finally, the roughening of the polymer/liquid interface could also be attributed to the pres-  
42 ence of TEA. The presence of weak surface-active molecules might help the formation of  
43 interfaces, increasing the actual roughness or lead to a larger SLD gradient upon adsorption,  
44 visible as an increased interface roughness (rather than a distinct layer) due to the small size  
45 of TEA.  
46  
47  
48  
49  
50  
51  
52  
53  
54  
55  
56  
57  
58  
59  
60

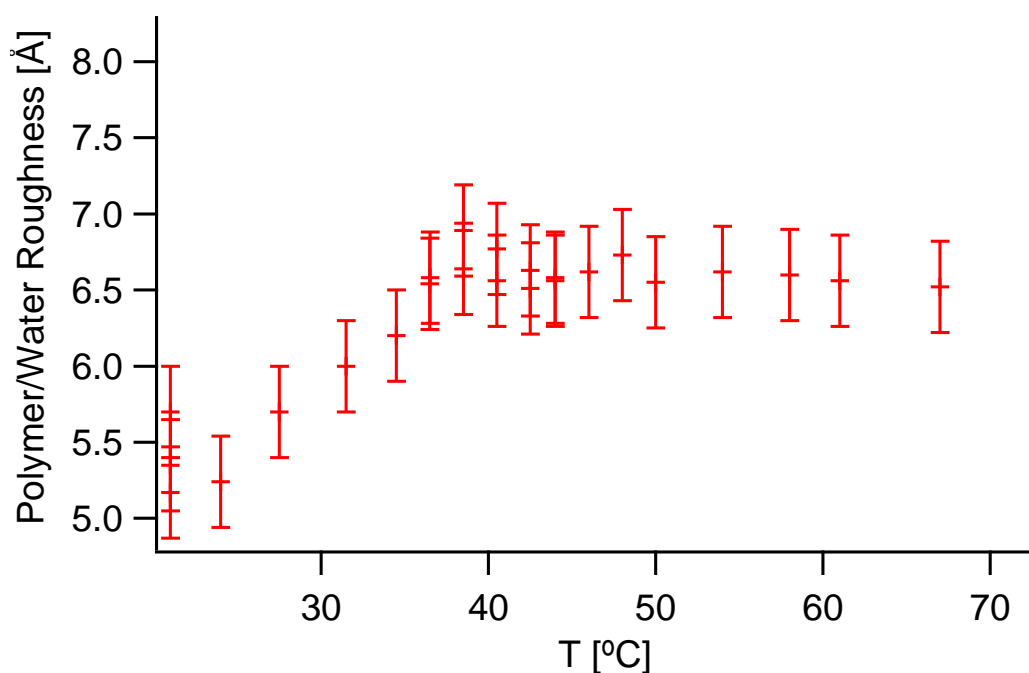


Figure 11: Roughness of the aqueous/polymer interface deduced from NR for a solution of 0.3%BA and 0.1% PTR-2 in D<sub>2</sub>O as a function of temperature.

For higher BA concentrations the roughness values are generally higher going up to 1.2 nm but show a similar increasing trend with temperature. Due to the limited temperature ranges available for the other BA concentrations and larger uncertainties their trends are not obvious and therefore they were not analyzed further.

## Temperature and solvent influence on the stability of the film

An important outcome of this experiment regarding art restoration field is the onset of film breaking and destruction. Indeed while increasing the temperature most of films investigated here, except for 0.3%, breaks within the NR experiment yielding a non quantifiable NR spectra. The critical temperature ( $T_{crit}$ ) for film breaking is found to to be BA fraction dependent and decreases with increasing BA from room temperature to above 72 °C (Fig. 12). At 0.3%, the film never breaks until the temperature limit of this study (16.5 to 73 °C). At 0.5%, the temperature of the film breaking was 72 °C, at 0.6% BA at 44 °C

1  
2  
3 and at 0.7% BA only at 21 °C.  
4

5 The basic idea behind the strategy of adding moieties of good solvent to a bad solvent gel in  
6 art restoration is softening the varnish film to promote its mechanical removal by abrasion.  
7 This would lead to reducing its  $T_g$  below room temperature via solvent plasticising. The re-  
8 sults presented here show that the mechanism is more complex and the chemical interaction  
9 plays an important role in this process.  
10  
11  
12  
13  
14

15 The  $T_g$  of the binary LA/BA mixture can be estimated using the partitioning constant of  
16 BA between LA and water from NR experiments on thin films<sup>14</sup> and the mixing model:  
17  
18  
19

$$\frac{1}{T_g} = \frac{1 - \phi_{BA}}{T_{g(LA)}} + \frac{\phi_{BA}}{T_{g(BA)}}, \quad (5)$$

20  
21  
22  
23

24 Using  $T_{g(BA)} = -105.15\text{ °C}$ <sup>59</sup> for BA and  $T_{g(LA)} = 47\text{ °C}$  for LA and the  $\phi_{BA/LA}$  concen-  
25 trations from our previous study.<sup>14</sup> The resulting glass transition temperature as a function  
26 of  $\Phi_{BA/WA}$  is plotted in Fig. 12 as a black line and decreases from around 35 °C at 0.3%  
27 BA to 18 °C at 0.7% BA, the highest solvent concentration examined in this study. The  
28 temperature at which a sudden increase in mass loss is observed (film removal) is at 44 °C  
29 for 0.6% BA, 72 °C for 0.5% BA and above 72 °C for 0.3% BA, which is 20-37 °C above the  
30 respective glass transition temperature. This suggests that the sudden 'unfreezing' of the  
31 film's surface tension stress is not the main motor for film breaking because at 0.3% and  
32 0.5% BA concentrations the film remains largely intact. This does not mean, however, that  
33 residual stresses cannot be the origin of hole nucleation as observed for other polymer thin  
34 films.<sup>60</sup>  
35  
36  
37  
38  
39  
40  
41  
42  
43  
44  
45

46 Another important outcome of the fact that the film remains largely intact for extended  
47 periods of time more than 20 °C above  $T_g$  is that the kinetics driving the film destruction  
48 are not controlled by the polymer viscosity. As LA is a low molecular weight polymer its  
49 viscosity should decrease by orders of magnitude when crossing  $T_g$ . If 'normal' dewetting,  
50 which kinetics are governed by viscosity, were to be the origin of film destruction in the here  
51  
52  
53  
54  
55  
56  
57  
58  
59  
60

1  
2  
3 studied case the kinetics should accelerate by orders of magnitude above  $T_g$  as observed with  
4 thin polystyrene films dewetting from functionalized silicon substrates: An acceleration of a  
5 factor 10 was observed when heating the sample by 10 °C above  $T_g$ .<sup>61</sup> In the here studied case  
6 the polymer film in contact with a co-polymer solution containing 0.3% BA was withstand-  
7 ing more than 10 h at temperatures significantly above  $T_g$  showing a clear layered structure  
8 observed by Kiessig fringes in the NR curves despite a high fraction of holes present. If,  
9 on the other hand, the BA concentration in the solution is increased to 0.7% the film is  
10 almost completely lost within only 3.5 h at 19 °C, which is around  $T_g$ . In essence, clearly the  
11 BA concentration inside the polymer is driving the kinetics of film destruction and not the  
12 polymers' viscosity.

13  
14  
15  
16  
17  
18  
19  
20  
21  
22  
23 The fact that the polymer softening is not the main driver for film break-up can also be  
24 appreciated by the concentration and temperature dependence of the different stages of film  
25 destruction. In Fig. 12 the information from  $T_g$  estimations, specular and off-specular NR  
26 on the state of the varnish film is summarized in a film stability diagram. The boundaries  
27 in this diagram are chosen to separate three regimes of film stability depending on  $\phi_{BA/W}$   
28 and temperature: a) The area below the black line corresponds to the solid zone below  $T_g$   
29 as calculated from eq. 5, b) At higher temperature the polymer is liquid but does not show  
30 pronounced hole formation as evidenced by low OSS intensity. It is chosen to separate this  
31 phase from the inhomogenous zone at higher temperatures by a threshold of Yoneda peak  
32 intensity of  $10^4$  counts per minute (see Fig. S4 in the supporting information), marked by  
33 a blue line. This choice is arbitrary but its exact value will only shift the temperature of  
34 the boundary keeping the qualitative behaviour with BA concentration the same. Finally,  
35 the red line marks the temperature at which a sudden loss of most of the film's material is  
36 observed.

37  
38  
39  
40  
41  
42  
43  
44  
45  
46  
47  
48  
49  
50  
51 Looking at this film stability diagram it is obvious that the boundaries of film destabilisa-  
52 tion are uncorrelated with the  $T_g$  evolution: While  $T_g$  is decreasing almost linearly with the  
53 BA concentration in the investigated range with a rather small slope, the other boundaries  
54  
55  
56  
57  
58  
59  
60

show a much steeper BA dependence and are not necessarily linear.

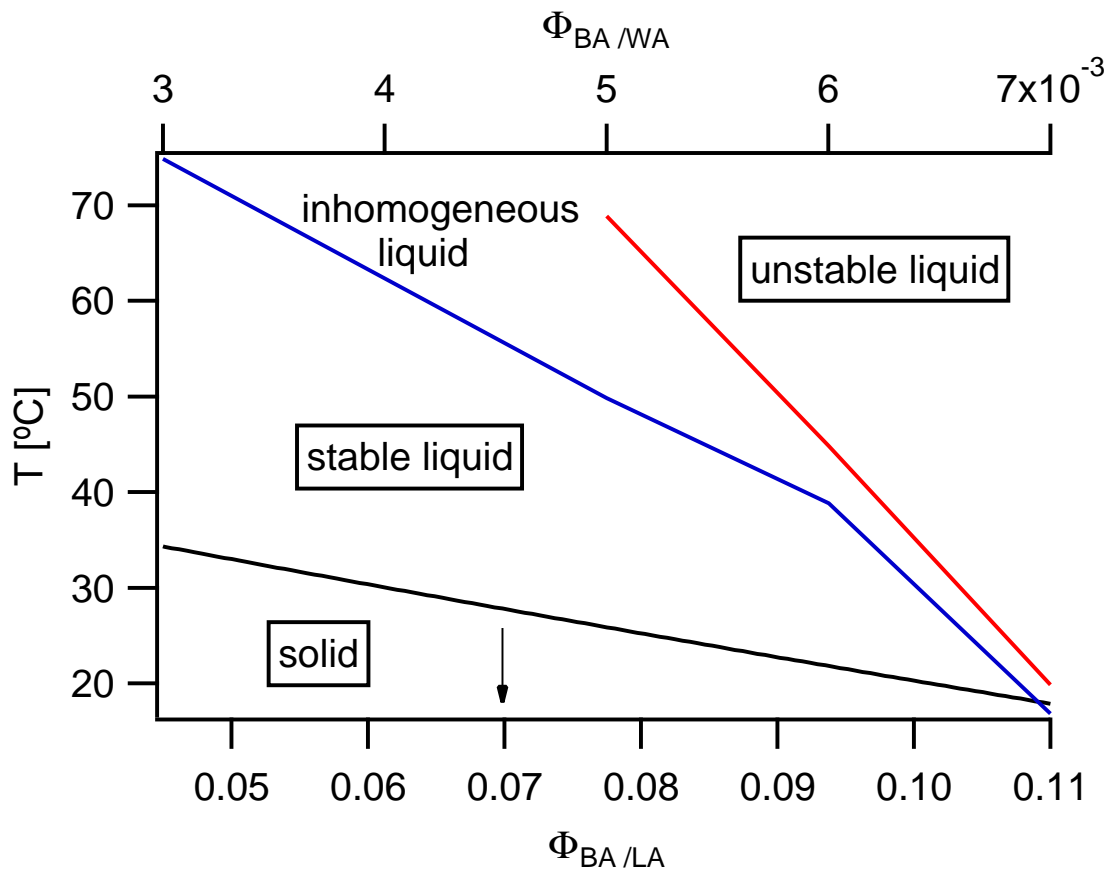


Figure 12: Film stability diagram using the  $T_g$  and NR results. The lower black line corresponds to the  $T_g$  as calculated from eq. 5 by using the BA in LA volume fractions from the bottom axis. The blue line in the middle corresponds to the threshold temperature where the OSS intensity is  $10^4$  counts per minute in Fig. S4 from the SI and the red line in the upper right corner marks the temperature at which a sudden loss of most of the film's material is observed. The latter two lines relate to the upper x-axis (BA fraction in water) and are deduced from the experimental data.

## Discussion

Given the clear indications that the appearance of water-filled holes growing with time is responsible for the here studied film destruction, dewetting might seem to be the most likely scenario. Moreover, a very similar behaviour of the scattering curves at late stages of film destruction, compared to the case of pure water where dewetting was observed, can be shown as evidenced in the Supporting information. Clearly the driving force is the hydrophilicity



1  
2  
3 of the used substrate attracting the polar emulsifier and/or water as observed in our pre-  
4 vious study.<sup>14</sup> The role of polar forces in dewetting of thin hydrophobic polymer films was  
5 also shown for polystyrene supported by silicon wafers immersed in poor solvents<sup>30</sup> or non  
6 solvent/poor solvent mixtures.<sup>31</sup>  
7  
8  
9  
10

11  
12  
13 However, several contradictions to the process of dewetting are observed. The most sig-  
14 nificant one is probably the fact that the kinetics are not governed by the polymer viscosity,  
15 but linked to the amount of solvent swelling. Clearly the retardation of dewetting is gradually  
16 switched off by increased solvent concentration inside the polymer. Suppression of dewetting  
17 was already observed for thin polystyrene films when their chain ends were functionalized  
18 by polar groups, explained by their bonding to the polar substrate and between the chains  
19 stabilizing the film.<sup>29</sup> Laropal is known to incorporate a significant amount of polar groups  
20 as well<sup>40</sup> and in our previous study of LA films in contact with water/BA mixtures we ob-  
21 served a wetting layer which was not perforated by the dewetting holes testifying the strong  
22 bonding of annealed LA to the polar substrate.<sup>14</sup> However, at higher BA concentrations or  
23 longer exposure the vast majority of the film vanished, eventually. In the aforementioned  
24 study we also observed a retarded swelling of the LA film when exposed to aqueous solu-  
25 tions containing increasing amounts of BA: While for small solvent concentrations almost  
26 no swelling was observed, a linear swelling behaviour was recovered as predicted for bulk LA  
27 at BA concentrations above 0.2%. We argued that bonding or cross-linking of some sites of  
28 the polymer to the substrate were responsible for this swelling retardation, which would be  
29 gradually suppressed by the addition of BA.  
30  
31  
32  
33  
34  
35  
36  
37  
38  
39  
40  
41  
42  
43  
44  
45  
46  
47  
48

49 It is possible that a similar mechanism is at play in the here studied case of the same LA  
50 film in contact with a BA containing viscous polymer dispersion. Indeed, for 0.3% BA we  
51 again observe a quasi water-free zone close to the substrate (see Fig. 3 Bottom) although  
52 this 'wetting layer' is much less pronounced compared to our previously investigated case  
53  
54  
55  
56  
57  
58  
59  
60

1  
2  
3 without the Pemulen. In addition, contrary to our previous study, at higher BA concen-  
4 trations this 'dry' layer is not visible anymore. This could be, however, due to the much  
5 more polar -OH groups contained in the co-polymer in comparison to water. Therefore the  
6 scenario of dewetting retardation due to polar group interactions inside the polymer film and  
7 with the polar substrate, which are gradually screened or broken by the polar BA seems to  
8 be the most likely scenario. The highly stable film state could be also appreciated by a test  
9 where *in situ* shear was applied to the BA swollen film not altering its structure as shown  
10 in the supplementary information.  
11  
12  
13  
14  
15  
16  
17  
18  
19  
20

21 Another contradiction with typical dewetting (and the previous study on binary wa-  
22 ter/solvent systems) is the here observed absence of rims. However, this could be explained  
23 by a) the fact that the polymer/substrate interaction is effectively weaker due to the presence  
24 of highly charged groups of the Pemulen, similar to the absence of rims observed for films  
25 experiencing plug flow,<sup>62</sup> b) the smaller size of holes, similar to early stages of dewetting  
26 of polymer films on non-adsorbing substrates,<sup>28</sup> or most importantly c) the fact that the  
27 films are effectively fluid, being above the  $T_g$  while the dewetting speed is retarded and thus  
28 not limited by viscosity giving the films the time to reach their equilibrium thickness at any  
29 stage of dewetting.  
30  
31  
32  
33  
34  
35  
36  
37  
38  
39  
40

41 Due to the presence of an emulsifier in the system (Pemulen TR-2) we cannot exclude a  
42 gradual emulsification of the LA film by its incorporation into the aqueous phase due to the  
43 hydrophobic side groups of Pemulen, leaving behind voids leading to holes in the film. Due  
44 to the high viscosity of the solution it is technically challenging to establish an equilibrium  
45 phase diagram of the here studied system in contrast to the water-based system studied  
46 before.<sup>14</sup> However, Pemulen TR-2 is known to form a microgel with typical droplet sizes in  
47 the (sub-)micron range when stabilizing an emulsion.<sup>33</sup> Therefore an emulsification process  
48 starting from the polymer/gel interface should engender a significant roughening of the poly-  
49  
50  
51  
52  
53  
54  
55  
56  
57  
58  
59  
60

1  
2  
3 mer surface. As seen in Fig. 11 the measured polymer film roughness for a BA concentration  
4 of 0.3% never exceeds 1 nm testifying a molecularly smooth layer just before film rupture.  
5  
6 We note that the amount of benzyl alcohol inside the Pemulen solution was up to 0.7% in  
7 the current study that is significantly lower than the solubility limit in water (4%). We  
8 therefore expect the solvent to be homogeneously distributed as is the case in pure water.  
9  
10 Finally, the presence of TEA being a weak surface-active molecule might help the formation  
11 of interfaces and intermediate steps in the first stages of dewetting, kinetically favoring the  
12 process leading to the observed higher coverage of smaller holes.  
13  
14  
15  
16  
17  
18  
19  
20

21 On an application level, the results of this paper, such as the presence of holes or the  
22 temperature effect, provide new information for painting conservators and restorers. In  
23 case the holes pierce the entire varnish layer, the penetration of the solvent contained in  
24 the Wolbers gel can reach and get into the paint layer. Thus, inducing an irreversible  
25 risk of deformation, swelling and dissolution of this fragile layer. The appearance of (sub-  
26 )micron sized holes would also reduce the transparency of the coating. It has to be noted,  
27 however, that the here used silicon substrate is slightly hydrophilic and thus not generally  
28 representative for the pictorial layer supporting the varnish, being typically hydrophobic.  
29  
30 Nonetheless, deeper layers in an easel painting can be hydrophilic as the glue typically used  
31 to support the preparation. This could be exposed to the varnish in cases of cracks. Another  
32 difference in real paintings is of course the absence of sharp boundaries between the layers.  
33 These gradual boundaries have a stabilizing effect on film cohesion.  
34  
35  
36  
37  
38  
39  
40  
41  
42  
43  
44

45 On the other hand, the results of the combined action of temperature and solvent show that  
46 it is possible to remove varnish without mechanical stress, as is currently the case. Now,  
47 restorers have a better understanding of the process of removing varnish from paintings using  
48 solvent-loaded gels and can re-evaluate this approach in order to guarantee the safety of the  
49 paint layer.  
50  
51  
52  
53  
54  
55  
56  
57  
58  
59  
60

## Conclusion

The above results on the destruction of Laropal®A81 films in contact with solvent containing viscous polymer dispersions clearly show striking similarities with binary solvent/non-solvent mixtures studied earlier,<sup>14</sup> which points towards a dewetting-type process in the here studied system as well. As in the former case the appearance of water-filled cavities in the film is initiated by the addition of good solvent and significantly accelerated if the amount of solvent is increased. An increase in temperature above  $T_g$ , in turn, is not accelerating the dewetting kinetics as much, clearly showing that the dewetting speed is not viscosity limited as it is the case for pure non-polar polymers pointing towards a retardation of film destruction as seen for polymers having polar groups incorporated.<sup>29</sup> It is argued that the addition of polar solvent is screening or breaking the polar interactions inside the film and/or with the polar substrate leading to accelerated film destruction. Another similarity to the pure water case is the loss of polymer mass at late stages of dewetting.

There are, however, significant differences in the here studied case of a gelly matrix in comparison to the dewetting of Laropal®A81 in binary mixtures: No rims are observed, no clear wetting layer is seen and the size of the holes is significantly smaller, although their volume fraction is similar inside the layer. The smaller size of the holes and thus larger hole density can be explained by an increased spreading coefficient of the gel on the Si substrate due to the presence of highly charged -OH groups from the gel. It was shown that the hole density in dewetting polystyrene films on treated Si substrates is larger when in contact with higher energy surfaces.<sup>63</sup> The smaller size of the holes in turn partially explains why no rim is visible as the rim is not present for holes at early stages of visco-elastic film dewetting from non-adsorbing substrates<sup>28,64</sup>. In this case the altered interaction at the polymer/solid interface could be also the reason why no wetting layer is observed. Another explanation for the absence of rims could be the fluid nature of the film as the dewetting speed is obviously not viscosity limited.

In summary, the destruction of LA varnish films as used in art restoration when in contact

1  
2  
3 with Pemulen TR-2 aqueous solutions containing small amounts of solvent is not principally  
4 driven by reduction of the polymer's  $T_g$  but clearly governed by the good solvent swelling.  
5 The destruction is clearly occurring by the appearance of water-filled holes, similar to the  
6 previously reported dewetting-type process of the same films in binary solvent/non-solvent  
7 mixtures. Obviously, this behaviour would be catastrophic for art-restoration, it has to be  
8 noted, though, that the here used support (silicon) is hydrophilic, while the surfaces sup-  
9 porting the protective varnish layers in easel paintings are typically hydrophobic. However,  
10 the presence of polar groups inside Laropal®A81 seems to play a determining role for film  
11 stability, which is gradually screened by addition of polar solvent. This brings to evidence  
12 the importance of polar interactions in LA film removal, which should be taken into account  
13 in restoration recipes.  
14  
15  
16  
17  
18  
19  
20  
21  
22  
23  
24

25 The presence of the gellifying polymer, however, apparently changes the interface width  
26 between the varnish and the polymer solution without shifting the solvent partition in the  
27 bulk of the materials. This opens a way for art restoration to tune the chemical and surface  
28 interactions, not only by varying the concentrations of the involved materials but notably  
29 by changing temperature. This is potentially a way to make varnish removal safe for art  
30 restoration by the use of gels in a temperature-controlled way. The smaller size of the holes  
31 can be also less evident concerning optical distortions.  
32  
33  
34  
35  
36  
37  
38  
39  
40

## 41 Acknowledgement

42  
43  
44 We thank the ILL for neutron beam time on FIGARO (doi.ill.fr/10.5291/ILL-DATA.1-03-  
45 36). We thank the Partnership for Soft Condensed Matter at ILL for the use of compli-  
46 mentary techniques. The Laboratoire de Rhéologie et Procédés is part of the LabEx Tec 21  
47 (Investissements d'Avenir - grant agreement n° ANR-11-LABX-0030) and of the PolyNat  
48 Carnot Institut (Investissements d'Avenir - grant agreement n° ANR-11-CARN-030-01).  
49  
50  
51  
52  
53  
54  
55  
56  
57  
58  
59  
60

## Supporting Information Available

Additional NR fitting results, pre-characterization of LA layers, comparison of NR and OSS between LA films in contact with gel and pure water containing high BA concentrations and additional optical micrographs of LA films after long exposure to pure water and BA. *In situ* Rheo-NR of BA swollen LA films in contact with gel+BA.

## References

- (1) Debnath, K.; Bucio, T. D.; Al-Attili, A.; Khokhar, A. Z.; Saito, S.; Gardes, F. Y. Photonic crystal waveguides on silicon rich nitride platform. *Optics express* **2017**, *25*, 3214–3221.
- (2) Crudden, C. M.; Horton, J. H.; Narouz, M. R.; Li, Z.; Smith, C. A.; Munro, K.; Baddeley, C. J.; Larrea, C. R.; Drevniok, B.; Thanabalasingam, B., et al. Simple direct formation of self-assembled N-heterocyclic carbene monolayers on gold and their application in biosensing. *Nature communications* **2016**, *7*, 1–7.
- (3) Teh, L.; Tan, N.; Wong, C.; Li, S. Growth imperfections in three-dimensional colloidal self-assembly. *Applied Physics A* **2005**, *81*, 1399–1404.
- (4) Boissière, C.; Grosso, D.; Prouzet, E. Inorganic Nanomaterials Synthesis Using Liquid Crystals. *Encyclopedia of Inorganic Chemistry* **2006**,
- (5) Stolow, N. Action of solvents on dried linseed oil films. *Nature* **1957**, *179*, 579.
- (6) Stolow, N. The measurement of film thickness and of solvent action on supported films. *Studies in Conservation* **1957**, *3*, 40–44.
- (7) Michalski, S. A physical model of the cleaning of oil paint. *Studies in Conservation* **1990**, *35*, 85–92.

- 1  
2  
3 (8) Phenix, A.; Sutherland, K. The cleaning of paintings: effects of organic solvents on oil  
4 paint films. *Studies in Conservation* **2001**, *46*, 47–60.  
5  
6  
7  
8 (9) Fife, G. R.; Stabik, B.; Kelley, A. E.; King, J. N.; Blümich, B.; Hoppenbrouwers, R.;  
9 Meldrum, T. Characterization of aging and solvent treatments of painted surfaces using  
10 single-sided NMR. *Magnetic Resonance in Chemistry* **2015**, *53*, 58–63.  
11  
12  
13  
14 (10) Brandi, C.; Déroche, C. *Théorie de la restauration*; École nationale du patrimoine,  
15 2001.  
16  
17  
18  
19 (11) Stolow, N. Application of science to cleaning methods: Solvent action studies on pig-  
20 mented and unpigmented linseed oil films. *Studies in Conservation* **1961**, *6*, 84–88.  
21  
22  
23  
24 (12) Graham, I. The effect of solvents on linoxyn films. *F. Oil Col* **1953**, *36*, 500–500.  
25  
26  
27 (13) Carretti, E.; Bonini, M.; Berrie, L. D. B.-H.; Angelova, L.-V.; Baglioni, P.; Weiss, R.-G.  
28 New frontiers in Materials Science for Art Conservation: Responsive Gels and Beyond.  
29 *Accounts of Chemical Research* **2010**, *43*, 751–760.  
30  
31  
32  
33 (14) Castel, A.; Gutfreund, P.; Cabane, B.; Rharbi, Y. Swelling, dewetting and breakup in  
34 thin polymer films for cultural heritage. *Soft Matter* **2020**,  
35  
36  
37  
38 (15) Wolbers, R. *Cleaning painted surfaces: aqueous methods*; 2000.  
39  
40  
41 (16) Bertolucci, S.; Bianchini, E.; Biave, C.; Caliari, F.; Cremonesi, P.; Gravina, S.; Zam-  
42 mataro, M.; Zangani, B. Preparazione e utilizzo di soluzioni acquose addensate, reagenti  
43 per la pulitura di opere policrome. *Progetto restauro* **2001**, *7*, 28–33.  
44  
45  
46  
47 (17) Sun, M.; Zou, J.; Zhang, H.; Zhang, B. Measurement of reversible rate of conservation  
48 materials based on gel cleaning approach. *Journal of Cultural Heritage* **2015**, *16*, 719–  
49 727.  
50  
51  
52  
53  
54  
55  
56  
57  
58  
59  
60

- 1  
2  
3 (18) Guizzo, S.; Tortolini, C.; Pepi, F.; Leonelli, F.; Mazzei, F.; Di Turo, F.; Favero, G.  
4 Application of microemulsions for the removal of synthetic resins from paintings on  
5 canvas. *Natural product research* **2016**, 1–11.  
6  
7  
8  
9  
10 (19) Rodriguez, S. H. Les propriétés, actions et principales problématiques des gels de  
11 Pemulen® TR-2. Le choix de la base dans la formulation des gels. CeROArt. Con-  
12 servation, exposition, Restauration d'Objets d'Art. 2017.  
13  
14  
15  
16 (20) Salama, K. K.; Ali, M. F.; El-Sheikh, M. S. The Conservation of an Egyptian Coptic  
17 Fresco Painting from Saint Jeremiah Monastery: The Use of Nano-Materials in Cleaning  
18 and Consolidation. *Journal of Nano Research*. 2017; pp 148–153.  
19  
20  
21  
22  
23 (21) Baglioni, P.; Berti, D.; Bonini, M.; Carretti, E.; Dei, L.; Fratini, E.; Giorgi, R. Micelle,  
24 microemulsions, and gels for the conservation of cultural heritage. *Advances in Colloid*  
25 *and Interface Science* **2014**, *205*, 361–371.  
26  
27  
28  
29  
30 (22) Chelazzi, D.; Giorgi, R.; Baglioni, P. Microemulsions, micelles, and functional gels:  
31 how colloids and soft matter preserve works of art. *Angewandte Chemie International*  
32 *Edition* **2018**, *57*, 7296–7303.  
33  
34  
35  
36  
37 (23) Singh, A.; Mukherjee, R. Swelling Dynamics of Ultrathin Polymer Films. *Macro-*  
38 *molecules* **2003**, *36* (23), 8728–8731.  
39  
40  
41  
42 (24) Miller-chou, B.-A.; Koenig, J.-L. A review of polymer dissolution. *Progress in Polymer*  
43 *science* **2003**, *28* (8), 1223–1270.  
44  
45  
46  
47 (25) Ellison, C.-J.; Torkelson, J.-M. The distribution of glass-transition temperatures in  
48 nanoscopically confined glass formers. *Nature Materials* **2003**, *2*(10), 695–701.  
49  
50  
51  
52 (26) Nieto Simavilla, D.; Huang, W.; Housmans, C.; Sferrazza, M.; Napolitano, S. Tam-  
53 ing the Strength of Interfacial Interactions via Nanoconfinement. *ACS Central Science*  
54 **2018**, *4*, 755–759.  
55  
56  
57  
58  
59  
60



- 1  
2  
3 (27) Seemann, R.; Herminghaus, S.; Neto, C.; Schlagowski, S.; Podzimek, D.; Konrad, R.;  
4 Mantz, H.; Jacobs, K. Dynamics and structure formation in thin polymer melt films.  
5 *Journal of Physics: Condensed Matter* **2005**, *17*, S267–S290.  
6  
7  
8  
9  
10 (28) Reiter, G. Dewetting of highly elastic thin polymer films. *Physical Review Letters* **2001**,  
11 *87*, 186101.  
12  
13  
14 (29) Henn, G.; Bucknall, D. G.; Stamm, M.; Vanhoorne, P.; Jérôme, R. Chain End Effects  
15 and Dewetting in Thin Polymer Films. *Macromolecules* **1996**, *29*, 4305–4313.  
16  
17  
18 (30) Xu, L.; Sharma, A.; Joo, S. W. Dewetting of Stable Thin Polymer Films Induced by a  
19 Poor Solvent: Role of Polar Interactions. *Macromolecules* **2012**, *45*, 6628–6633.  
20  
21  
22 (31) Xu, L.; Sharma, A.; Joo, S. W.; Liu, H.; Shi, T. Unusual Dewetting of Thin Polymer  
23 Films in Liquid Media Containing a Poor Solvent and a Nonsolvent. *Langmuir* **2014**,  
24 *30*, 14808–14816, PMID: 25402851.  
25  
26  
27 (32) Simovic, S.; Tamburic, S.; Milic-Askabic, J.; Rajic, D. An investigation into interac-  
28 tions between polyacrylic polymers and a non-ionic surfactant: an emulsion preformu-  
29 lation study. *International Journal of Pharmaceutics* **1999**, *184*, 207 – 217.  
30  
31  
32 (33) Szűcs, M.; Sandri, G.; Bonferoni, M. C.; Caramella, C. M.; Vaghi, P.; Szabó-Révész, P.;  
33 Erős, I. Mucoadhesive behaviour of emulsions containing polymeric emulsifier. *European*  
34 *journal of pharmaceutical sciences* **2008**, *34*, 226–235.  
35  
36  
37 (34) Feller, R.-L.; Stolow, N.; Jones, E.-H. In *On picture varnishes and their solvents. Revised*  
38 *and enlarged edition*; National Gallery of Art distributed by The Foundation of the  
39 American Institute for Conservation of Historic,, Works, A., Eds.; 1971.  
40  
41  
42 (35) Diethert, A.; Metwalli, E.; Meier, R.; Zhong, Q.; Campbell, R.-A.; Cubitt, R.; Müller-  
43 Buschbaum, P. In situ neutron reflectometry study of the near-surface solvent concen-  
44 tration profile during solution casting. *Soft Matter* **2011**, *7* (2-3), 6648–6659.  
45  
46  
47  
48  
49  
50  
51  
52  
53  
54  
55  
56  
57  
58  
59  
60

- 1  
2  
3 (36) Michalski, S. A physical model of the cleaning of oil paint. *Studies in Conservation*  
4 **1990**, *35:sup1*, 85–92.  
5  
6  
7  
8 (37) Wolff, M.; Kuhns, P.; Liesche, G.; Ankner, J. F.; Browning, J. F.; Gutfreund, P. Com-  
9 bined neutron reflectometry and rheology. *Journal of Applied Crystallography* **2013**,  
10 *46*, 1729–1733.  
11  
12  
13  
14  
15 (38) <https://www.basf.com>.  
16  
17  
18 (39) la Rie, E. D.; Lomax, S.; Palmer, M.; Glinsman, L.; Christopher, A. An investiga-  
19 tion of the photochemical stability of urea-aldehyde resin retouching paints. *Studies in*  
20 *Conservation* **2000**, *45:sup1*, 51–59.  
21  
22  
23  
24 (40) Bonaduce, I.; Colombini, M.; I.Degano,; Girolamo, F. D.; Nasa, J. L.; Modugno, F.;  
25 Orsini, S. Mass spectrometric techniques for characterizing low-molecular-weight resins  
26 used as paint varnishes. *Analytical and Bioanalytical Chemistry* **2012**, *405 (2-3)*, 1047–  
27 1065.  
28  
29  
30  
31  
32  
33 (41) Maines, C. A.; la Rie, E. D. Size-exclusion chromatography and differential scanning  
34 calorimetry of low molecular weight resins used as varnishes for paintings. **2004**, *52*,  
35 39–45.  
36  
37  
38  
39  
40 (42) <http://www.ctseurope.com>.  
41  
42  
43 (43) Madsen, F.; Eberth, K.; Smart, J. D. A rheological assessment of the nature of inter-  
44 actions between mucoadhesive polymers and a homogenised mucus gel. *Biomaterials*  
45 **1998**, *19*, 1083–1092.  
46  
47  
48  
49  
50 (44) Ravenel, N. Pemulen® TR-2: An Emulsifying Agent with Promise. *WAAC Newsletter*  
51 *Volume* **2010**, *32*, 10–12.  
52  
53  
54 (45) Shahin, M.; Hady, S. A.; Hammad, M.; Mortada, N. Optimized formulation for topical  
55  
56  
57  
58  
59  
60

- 1  
2  
3 administration of clotrimazole using Pemulen polymeric emulsifier. *Drug development*  
4 *and industrial pharmacy* **2011**, *37*, 559–568.  
5  
6  
7
- 8 (46) Hall, D. B.; Underhill, P.; Torkelson, J. M. Spin coating of thin and ultrathin polymer  
9 films. *Polymer Engineering & Science* **1998**, *38*, 2039–2045.  
10  
11
- 12 (47) Campbell, R. A.; Wacklin, H. P.; Sutton, I.; Cubitt, R.; Fragneto, G. FIGARO: The  
13 new horizontal neutron reflectometer at the ILL. *Eur. Phys. J. Plus* **2011**, *126*.  
14  
15
- 16 (48) Gutfreund, P.; Saerbeck, T.; Gonzalez, M. A.; Pellegrini, E.; Laver, M.; Dewhurst, C.;  
17 Cubitt, R. Towards generalized data reduction on a chopper-based time-of-flight neu-  
18 tron reflectometer. *Journal of Applied Crystallography* **2018**, *51*, 606–615.  
19  
20  
21  
22
- 23 (49) Abelès, F. Recherches sur la propagation des ondes électromagnétiques sinusoïdales  
24 dans les milieux stratifiés-Application aux couches minces. *Annales de physique*. 1950;  
25 pp 596–640.  
26  
27  
28  
29
- 30 (50) Nelson, A. Co-refinement of multiple-contrast neutron/X-ray reflectivity data using  
31 MOTOFIT. *Journal of Applied Crystallography* **2006**, *39*, 273–276.  
32  
33  
34
- 35 (51) <https://refl1d.readthedocs.io/en/latest/>.  
36  
37
- 38 (52) <https://www.ncnr.nist.gov/resources/activation/>.  
39  
40
- 41 (53) Lauter, V.; Lauter, H.; Glavic, A.; Toperverg, B. Reference module in materials science  
42 and materials engineering. 2016.  
43  
44  
45
- 46 (54) Hafner, A. Full Off-Specular and Specular Reflectometry for Soft Thin Film Analysis.  
47 Ph.D. thesis, Université libre de Bruxelles, Faculté des Sciences – Physique, Bruxelles,  
48 2019.  
49  
50  
51  
52
- 53 (55) de Gennes, P. G. Dynamics of fluctuations and spinodal decomposition in polymer  
54 blends. *The Journal of Chemical Physics* **1980**, *72*, 4756–4763.  
55  
56  
57  
58

- 1  
2  
3 (56) Sferrazza, M.; Heppenstall-Butler, M.; Cubitt, R.; Bucknall, D.; Webster, J.; Jones, R.  
4 A. L. Interfacial Instability Driven by Dispersive Forces: The Early Stages of Spinodal  
5 Dewetting of a Thin Polymer Film on a Polymer Substrate. *Physical Review Letters*  
6 **1998**, *81*, 5173–5176.  
7  
8  
9  
10  
11  
12 (57) Good, R. J.; Girifalco, L. A. A THEORY FOR ESTIMATION OF SURFACE AND IN-  
13 TERFACIAL ENERGIES. III. ESTIMATION OF SURFACE ENERGIES OF SOLIDS  
14 FROM CONTACT ANGLE DATA. *The Journal of Physical Chemistry* **1960**, *64*, 561–  
15 565.  
16  
17  
18  
19  
20  
21 (58) Braslau, A.; Deutsch, M.; Pershan, P. S.; Weiss, A. H.; Als-Nielsen, J.; Bohr, J. Surface  
22 Roughness of Water Measured by X-Ray Reflectivity. *Phys. Rev. Lett.* **1985**, *54*, 114–  
23 117.  
24  
25  
26  
27  
28 (59) Tylinski, M.; Chua, Y.; Beasley, M.; Schick, C.; Ediger, M. Vapor-deposited alcohol  
29 glasses reveal a wide range of kinetic stability. *The Journal of chemical physics* **2016**,  
30 *145*, 174506.  
31  
32  
33  
34  
35 (60) Reiter, G.; Hamieh, M.; Damman, P.; Sclavons, S.; Gabriele, S.; Vilmin, T.; Raphaël, E.  
36 Residual stresses in thin polymer films cause rupture and dominate early stages of  
37 dewetting. *Nature materials* **2005**, *4*, 754–758.  
38  
39  
40  
41  
42 (61) Bäumchen, O.; Fetzer, R.; Jacobs, K. Reduced Interfacial Entanglement Density Affects  
43 the Boundary Conditions of Polymer Flow. *Physical Review Letters* **2009**, *103*, 247801.  
44  
45  
46  
47 (62) Debrégeas, G.; Martin, P.; Brochard-Wyart, F. Viscous bursting of suspended films.  
48 *Physical review letters* **1995**, *75*, 3886.  
49  
50  
51  
52 (63) Ashley, K. M.; Meredith, J. C.; Amis, E.; Raghavan, D.; Karim, A. Combinatorial  
53 investigation of dewetting: polystyrene thin films on gradient hydrophilic surfaces.  
54 *Polymer* **2003**, *44*, 769 – 772.  
55  
56  
57  
58  
59  
60

- 1  
2  
3 (64) Brochard-Wyart, F.; Debregeas, G.; Fondcave, R.; Martin, P. Dewetting of Supported  
4  
5 Viscoelastic Polymer Films: Birth of Rims. *Macromolecules* **1997**, *30*, 1211–1213.  
6  
7  
8  
9  
10  
11  
12  
13  
14  
15  
16  
17  
18  
19  
20  
21  
22  
23  
24  
25  
26  
27  
28  
29  
30  
31  
32  
33  
34  
35  
36  
37  
38  
39  
40  
41  
42  
43  
44  
45  
46  
47  
48  
49  
50  
51  
52  
53  
54  
55  
56  
57  
58  
59  
60

## Graphical TOC Entry

